cis-Cytokinins from the tRNA-degradation pathway impact the phenotype and metabolome of _Arabidopsis thaliana:_ evidence from AtIPT2 and AtIPT9 null mutants

A thesis submitted to the committee on Graduate Studies
in partial fulfillment of the requirements for the degree of Master of Science
in the Faculty of Arts and Science

Trent University

Peterborough, Ontario, Canada

Environmental and Life Sciences M.Sc. Graduate Program

January 2019

Abstract

cis-Cytokinins from the tRNA-degradation pathway impact the phenotype and metabolome of *Arabidopsis thaliana:* evidence from AtIPT2 and AtIPT9 null mutants

Cody Butler

Cis-isomers of the cytokinin plant hormone family are thought to have low activity or impact on plant growth and development. Mutants with independent silencing of the pathway leading to cis-CK (cis-cytokinin) were investigated at the phenotype and metabolite levels. Phenotypic deviations were noted in trichome development, fresh weight, rosette diameter, number of non-rosette leaves, shoot height, delayed flowering, flower number, and carotenoids. Exploratory metabolomic analysis detected a number of metabolite features that have been associated with CK, auxin, and ABA (abscisic acid) activity. Evidence from both phenotype and metabolomic analysis support the hypothesis that *cis*-CK production is biologically important for plant growth and development.

Acknowledgements

I would like to thank my supervisor Dr. Neil Emery his guidance on my journey into plant sciences and beyond. I would also like to thank Dr. Ewa Cholewa of Nipissing University for introducing me to plant sciences as an undergrad, and all your help introducing me to Dr. Emery. I wouldn't be where I am without you both. I would also like to thank my committee members Dr. Naomi Stock, and Dr. David Ellis. Your insight and guidance along this journey kept me on track, and made my foray into metabolomics much, much smoother. Jake Lyne, I appreciate all your help with planting, growth, measurements, pictures, and sampling. You noticed minute details that rounded out the phenotype data, that I may have overlooked otherwise. I also need to thank all the members of the Emery lab. Each one of you has helped me in some way, whether you know it or not. It was a pleasure working alongside all of you. Last but certainly not least, I owe a big thank you to Dr. Anna Kisiala. You've never let me be anything less than my best. I have the utmost respect and admiration for you as a researcher, and as person. This project would not have come to fruition without your help.

Table of Contents

List of Figures and Tables

Figures

Tables

Summary of Abbreviations

ABA	Abscisic acid
AtIPT2	*Arabidopsis thaliana* isopentenyltransferase 2
AtIPT9	*Arabidopsis thaliana* isopentenyltransferase 9
CKs	Cytokinins
cZ	*cis*-Zeatin
DZ	Dihydrozeatin
DMAPP	Dimethylallyl diphosphate
HMDBP	4-hydroxy-3-methyl-2-(E)-butenyl diphosphate
ITC	Isothiocyanate
LC-MS/MS	Liquid chromatography-mass spectrometry/mass spectrometry
MEP	Methylerythritol phosphate
NAD	Nicotinamide Adenine Dinucleotide
2MeS	Methylthiol
MVA	Mevalonate
NCE	Normalized Collision Energy
PRM	Parallel Reaction Monitoring
tZ	*trans*-Zeatin
WT	Wild type

Chapter 1: Introduction

1.1 *Arabidopsis* as a model species

Arabidopsis thaliana (mouse ear cress) is a small flowering eudicot, indigenous to Europe. It is in the family Brassicaceae along with cabbage and mustard. Its close relation to some modern crops is one of the many reasons it is considered a model plant species in plant biological studies. In fact, it was the first plant to have its entire genome sequenced (The Arabidopsis Genome Initiative, 2000), and its growth and development has been documented in great detail (Boyes, 2001). Around the time the *Arabidopsis* genome was sequenced, there was an explosion of studies focused on cataloging genes and their function (Alonso et al., 2003; Bouché & Bouchez, 2001; Grotz et al., 1998; Maruyama et al., 2004; Xie, Feys, James, Nieto-Rostro, & Turner, 1998).

1.2 Cytokinins

Cytokinins (CKs) are evolutionally old and highly conserved low-mass molecules that have been identified in almost all known organisms (Spíchal, 2012). Although CKs are considered a class of phytohormones, their production and functions are not exclusive to plants and they have been documented to occur in a diverse group of organisms including bacteria, fungi (Morrison, Emery, & Saville, 2017), mammals (Seegobin et al., 2018) and humans (Golovko, Hjälm, Sitbon, & Nicander, 2000; Persson, Esberg, Ólafsson, & Björk, 1994; Spíchal, 2012; Stirk & van Staden, 2010). CKs are believed to be the central regulators of cell division and differentiation in plants (K. Miyawaki et al., 2006), and can act both locally and at a distance (Osugi & Sakakibara, 2015). They also control several metabolic processes including: flowering, fruit set, seed filling, inhibition of senescence, and many other related functions (Mok & Mok, 2001).

Chemically, cytokinins are derivatives of adenine, but cytokinin-like activity is also shown by some phenylurea derivatives (Frébort, Kowalska, Hluska, Frébortová, & Galuszka, 2011). Four basic forms of cytokinins occur naturally: isopentenyl adenine (iP), *trans*-zeatin (tZ), *cis*-zeatin (cZ) and dihydrozeatin (DZ) (Kamada-Nobusada & Sakakibara, 2009). CKs are commonly present as free bases (FB), ribosides (RB) or nucleotides (NT). FB are the most active type, RB are thought to be transport and signaling types (Hirose et al., 2008) while NT are inactive and believed to be more stable precursor forms (Sakakibara, 2006). CKs also exist as products of glucosylation as glucosides (GLUC) or methylthiolation as methylthiol (2MeS) –type derivatives, (Morrison et al., 2017).

Two pathways exist in cytokinin biosynthesis (Spíchal, 2012); the *de novo* pathway producing tZ type CKs, and the tRNA-degradation pathway producing cZ type CKs. A simplified pathway is shown below in Figure 1:

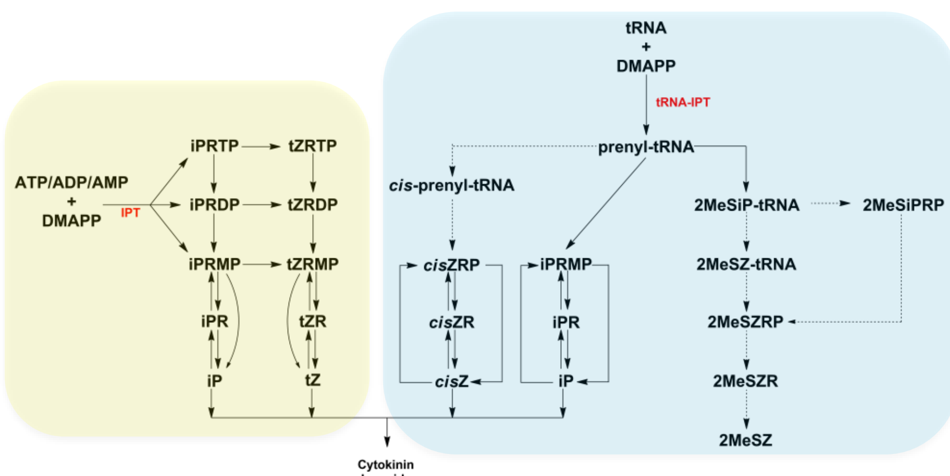

Figure 1: Simplified cytokinin biosynthesis pathway: de novo (yellow rectangle) catalyzed by IPT enzymes (highlighted red, left), and tRNA-degradation (blue rectangle) catalyzed by tRNA-IPT enzymes (highlighted red, right). (Adapted from Erin N. Morrison et al., 2015; Sakakibara, 2006).

In *Arabidopsis*, the *de novo* pathway is thought to be initiated and regulated by seven genes known as isopentenyltransferases (IPTs): AtIPT1, AtIPT3, AtIPT4, AtIPT5, AtIPT6, AtIPT7, and AtIPT8 (K. Miyawaki et al., 2006). These genes are homologous and are activated in response to cytokinin requirements in different tissues of *Arabidopsis* (Kaori Miyawaki, Matsumoto-Kitano, & Kakimoto, 2004). The location of the respective different gene activities varies, but the majority resides in plastids, with the exceptions of IPT7 in mitochondria and IPT4 in the cytosol (Skalický, Kubeš, & Napier, 2018).

Unlike the *de novo* pathway that is controlled by IPT enzymes, the tRNA-degradation pathway is catalyzed by two tRNA-specific isopentenyltransferases (tRNA-IPT), enzymes AtIPT2 and AtIPT9, (K. Miyawaki et al., 2006; Takei, Sakakibara, & Sugiyama, 2001), which produce *cis*-zeatin (cZ) and derivatives. The tRNA-degradation pathway is not exclusive to plants, and it is known to exist in bacteria (Scarbrough, Armstrong, Skoog, Frihart, & Leonard, 1973) and fungi (Strzelczyk , E., Pokojska, A., Kampert, M., Michalski, L., Kowalski, 1989), suggesting that is an evolutionarily ancient and prevalent pathway. This suggests that the tZ type CKs might be a new adaptation relative to the cZ type (Spíchal, 2012). A key difference between the two tRNA-IPT genes is that AtIPT2 enzymes are found in the cytosol of cells (Kasahara et al., 2004), while AtIPT9 enzymes are found in mitochondria and plastids (Sakakibara, personal communication, year). While the enzymes are found in different locations, tRNA-IPT genes are ubiquitously expressed in *Arabidopsis* tissues (Kaori Miyawaki et al., 2004).

The main purpose of the IPT and tRNA-IPT genes is the regulation of plant development by producing IPT enzymes, which catalyze the initial and rate limiting step in cytokinin production. This is done by the addition of an isoprenoid side chain to the N^6 amino group of adenine nucleotide (Lindner et al., 2014). Plants produce isoprenoid precursors via either the methylerythritol phosphate (MEP) pathway in plastids, or the mevalonate (MVA) pathway in the cytosol (Spíchal, 2012). The MVA pathway initially produces isopentenyl diphosphate, which can be isomerized to dimethylallyl diphosphate (DMAPP) (Frébort et al., 2011). The MEP pathway differs in that it produces 4-hydroxy-3-methyl-2-(E)-butenyl diphosphate (HMBDP), which can then be reduced into DMAPP, though at low levels. Both HMBDP and DMAPP can work as cytokinin precursors, but the level of HMBDP in plastids is much higher (Sakakibara et al., 2005), with its location indicating its use as a precursor for the *de novo* synthesis of CK.

The prenyl group used in tZ type CK synthesis arises primarily through the MEP pathway, and the production of the prenyl group for cZ type synthesis is dominated by the MVA pathway (Kasahara et al., 2004). However, because the MVA and MEP pathways can both produce DMAPP, it is possible a small amount produced by the MEP pathway can be used as a substrate for enzymes catalyzing tRNA-degradation and vice versa, despite being produced in two separate locations. In *Arabidopsis*, once CKs have been synthesized, they are detected through CK receptors localized mainly in the endoplasmic reticulum (Wulfetange et al., 2011). It was shown that cZ exhibits some activity at a receptor called CRE1/AHK4 (Spíchal et al., 2004; Tsutomu Inoue, Masayuki Higuchi, Yukari Hashimoto, Motoaki Seki, Masatomo Kobayashi, Tomohiko Kato, Satoshi Tabata, Kazuo Shinozaki, 2001) but it exhibits low sensitivity. Likewise, receptors AHK2 also AHK3 recognize cZ and DZ, but, again, they exhibit low sensitivity compared to tZ

(Gajdošová et al., 2011; Hwang & Sheen, 2001; Spíchal et al., 2004). This agrees with the fact that tZ is the dominant cytokinin isomer utilized in *Arabidopsis* metabolism (Gajdošová et al., 2011).

tZ and iP-type cytokinins are the most bioactive cytokinins; whereas, the *cis*-isomer was once widely thought to be present only in minor quantities and with low or no activity (Schmitz, Skoog, Playtis, & Leonard, 1972). While tZ was found to be a bioactive substance, cZ was reported to have a weak biological impact and, despite its derivatives being abundant in various plant materials, the biological role of *cis*-CK remained highly speculative (Hluska, 2017; Schäfer et al., 2015). However there are some plant species (many of them crops) in which *cis*-zeatin is the dominant cytokinin species such as potato (Mauk & Langille, 1978; Suttle & Banowetz, 2000), rice (Takagi, Yokota, Murofushi, Ota, & Takahashi, 1985), corn (Veach et al., 2003; Vyroubalova et al., 2009), chickpea (R.J. Neil Emery, Ma, & Atkins, 2000; Robert Joseph Neil Emery, Leport, Barton, Turner, & Atkins, 1998), pea (Quesnelle & Emery, 2007), and sweet potato (Hashizume et al., 1979) to name a few. This may be a result of the plant breeding process itself (Schäfer et al., 2015). It was previously suggested that cis-CKs might also play a role as a competitor to the more active CKs, thereby preserving specific CK functions that only require a low CK threshold (Gajdošová et al., 2011), this remains a possible function of cis-CK.

Recently cZ has become the focus of a few studies that have shown that cis-CKs can be active (Dello Ioio et al., 2012; Yonekura-Sakakibara, 2004). One such study involving IPT2 and IPT9 transgenic cotton showed that the timing of water deficit stress influences whether transgenic cotton has an advantage over WT cotton (Zhu et al., 2018). Likewise, in *Arabidopsis,* the only active CK enhanced under drought stress conditions was cZ, accompanied by an increase of its N- and O- glucosides (Prerostova et al., 2018). cZs may also play a role in regulating plant development and defense responses to pathogen and herbivore attack and highlight their potential role as "novel" stress-response markers (Schäfer et al., 2015). In addition, it was hypothesized that cZ-type CKs may act as delicate regulators of CK responses in plants under growth-limiting conditions (Gajdošová et al., 2011).

Since cytokinins are prominent as one of only a small few of major plant hormones which positively regulate most aspects of growth and development in higher plants, the importance of the different cytokinin pathways cannot be ignored. Although cZ is not the dominant isomer in *Arabidopsis*, in many crops such as rice and corn, cZ is the dominant isomer. It is a selective and energetic disadvantage for plants to use resources to synthesize metabolites they do not need. This would suggest that *tZ* has not completely replaced nor has it reduced *cis* zeatin to a negligible or redundant role, even in *Arabidopsis*. This raises the question - why does *Arabidopsis* bother to produce cZ when it is a *trans* dominated system? Are cCKs performing critical functions that could not be replicated by tZ, or are they evolutionary relics?

Hypothesis

The mounting evidence in recent studies by Gajdošová et al., 2011, Hluska 2017, and Schäfer et al., 2015 suggests that the tRNA-degradation pathway and *cis*-CK metabolites perform important functions. But this has not been adequately confirmed at phenotype level and it has never been studied at the metabolome level, where significant effects that are invisible at phenotype level can be detected. It is therefore hypothesized that *cis*-CK plays a biologically significant role in *Arabidopsis thaliana*, impacting both the phenotype and metabolism. It is therefore predicted that the levels of *cis*-CK, iP, 2MeS-CK, and ABA in IPT2 and IPT9 mutant should be reduced as these are the most likely cytokinins to be influenced by disruption of the tRNA-IPT degradation pathway. Subsequently this would have an effect on the development and growth of *Arabidopsis*, reflected in phenotypic deviations from WT (Wild type). The developmental metabolism of these plants would be altered as well, as reflected by changes in the metabolome of the mutant plants.

1.3 Phenotyping

The phenotype is the fundamental level for plant development. Simple phenotypic screens have played critical roles in the elucidation of phytohormone genetic pathways (Gazzarrini & Mccourt, 2003). The phenotype exhibited by a genetically modified plant can often be used to determine the effects that the deletion, addition, or silencing of a gene has caused. Sometimes the phenotypes are highly visible such as bioluminescent *Arabidopsis* (Alvarado et al., 2004), while others are subtle, which has been the case with AtIPT2 and AtIPT9 silencing. It was shown that basal leaves become chlorotic over time, as well as a shortened primary root, thought to be a result of the reduced root meristem size and ectopic protoxylem formation. (Köllmer, Novák, Strnad, Schmülling, & Werner, 2014; K. Miyawaki et al., 2006). This suggests an active role of cZ-CKs in growth and development of Arabidopsis and rice (Schäfer et al., 2015). However, beyond these basic leaf and root observations, no detailed phenotyping has been described. Therefore, a closer look at the phenotypes of these mutants will help determine what fundamental processes cZ may be influencing. Examining plant growth rate, masses, sizes, flowering, and characterizing minute changes to the structures of these mutants will provide further insight into the inner workings of the effects of cZ.

1.4 Metabolomics

Metabolomics is the study of the metabolite complement of an organism, or a cell, within a specific physiological condition. Plant metabolic studies were relatively neglected for a number of years, with more emphasis on human metabolism instead. However, recently there has been a resurgence in interest in plant metabolism. Increasing concerns about crop yield stability - particularly under the enhanced stresses that are anticipated with climate change (Leng & Huang, 2017), as well as the trend of searching for compounds that have significant impact against human disease (Ahn, 2017) are possible factors in the renewed interest. Many disciplines are moving toward the adoption of metabolomics as an effective form of analysis. This is partly due to the ability of metabolites to directly reflect the bioactivity and metabolism that is happening at the specific, snapshot in time of sample collection. In comparison to other "omics" type analyses, the analyte in question will typically only be present in biologically impactful concentrations when it is necessary or needed by the organism or tissue being explored. This is not always the case with the other 'omics' targets.

There are two branches of metabolomics - targeted and untargeted. Targeted typically involves knowing what type of specific metabolites one is looking for, while untargeted methods are usually used to determine the, yet unknown, significant metabolites that vary between samples or treatments. These newly discovered metabolites could then be targeted with tools such as tandem mass spectrometry to discover their identities. Untargeted metabolomic analysis aims at the identification and quantitation of all metabolites in a given biological sample (Weckwerth & Fiehn, 2002). It is important to consider the nature of extraction protocol one chooses when attempting to extract many metabolites because, unfortunately, no single analytical method is capable of extracting and detecting all metabolites (De Vos et al., 2007). For example, metabolic profiles of *Arabidopsis* extracts obtained with different solvents of different polarity were shown to be quite different (R. Verpoorte, 2007). In addition, the extraction process is time consuming and difficult to automate, and the addition of multiple sample clean-up steps that are usually required can introduce variability (Wu, Southam, Hines, & Viant, 2008). Plants are particularly diverse in metabolites, which are present in a wide range of concentrations. As such, identifying specific metabolites in untargeted studies is a challenge. Good extraction practices involve an optimized solvent system, and the rapid quenching of metabolism shortly after harvest; thus, skillful manipulation is required by the researcher.

To achieve invariant, unbiased metabolomic data, a well-thought-out sample preparation methodology is necessary. Tissue handling and wounding of plant tissue causes rapid metabolic activity, and must be stopped immediately, even after the tissue has been separated from the remainder of the plant. The most simple and succinct way to quench metabolism is to place samples in liquid nitrogen to snap-freeze them and carry out extraction and analyses shortly after harvest (R. Verpoorte, 2007). Water provides the medium for enzyme-mediated reactions which may occur during sample preparation, resulting in metabolite decomposition (R. Verpoorte, 2007), so the rapid freezing via liquid nitrogen or freeze drying prevents this from happening. That said, extracting frozen tissues that still contain the original amount of water at harvest might be advantageous for metabolomic approaches when compared to extracting freeze-dried samples, since freeze-drying may potentially lead to the irreversible adsorption of metabolites on cell walls and membranes (Weckwerth & Fiehn, 2002).

It is also important to keep in mind, when planning harvest times, that several primary metabolites can fluctuate following a diel cycle (Queiroz & Morel, 1974). Care must likewise be taken to harvest only the parts of a plant sample that one wishes to analyze, as metabolite concentrations can vary spatially among different organs and tissues (leaves, stems, roots etc.). Variation can also arise from procedural errors, natural biological variation, and metabolic activity after harvest of samples. Theoretically, if metabolomics was performed on a homozygous plant population, any variation found would indicate responses to subtle or even random differences in plant development or physiology for each individual plant (Weckwerth & Fiehn, 2002). Some examples are: working in a shared growing area may result in cross contamination of treatments applied to other experiments, spikes or dips in temperatures in the greenhouse, possible drought conditions due to neglect. Minimization of variation becomes increasingly important when elucidation of metabolite structures becomes the main objective. Currently, the number of metabolites present in the plant kingdom is estimated to exceed 200 000. Therefore, metabolomics approaches must apply adequate tissue sampling, homogenization, extraction, storage, and sample preparation methods to maintain an unbiased process (Weckwerth & Fiehn, 2002).

The selection of the instrumental technique for a particular metabolomic study depends on multiple factors, including: the accessibility to instrumentation, the specific questions at hand, as well as the training and background of the scientists involved. One of the main instrumental techniques in metabolomics is mass spectrometry (MS), which allows the detection of many metabolites simultaneously in complex mixtures, with little or no prior purification (Kerem Bingol, Lei Bruschweiler, Cao Yu, Arpad Somogyi, Fengli Zhang, 2016). Because of the sensitivity and selectivity of mass spectrometers in general, they have become the method of choice to characterize the human metabolome (Scalbert et al., 2009). This is also true in regard to the plant metabolome. Mass spectrometry is an analytical technique that measures the mass to charge ratio of particles introduced in a sample. With this information, the masses, elemental composition, and chemical structure can often be inferred. Mass spectrometry has earned a reputation as being a very quick and efficient way to detect many metabolites in a complex sample mixture, without purification. In discovery-based investigations, applying untargeted methods, thousands of metabolites can be detected with no or limited prior knowledge of the metabolite composition of samples (Dunn et al., 2013). A key development has been the availability of mass spectrometers that provide mass accuracy extending into the sub-5 ppm regime (Kerem Bingol, Lei Bruschweiler, Cao Yu, Arpad Somogyi, Fengli Zhang, 2016). This allows for confident detection and quantification of low concentration analytes, such as cytokinins.

With the incorporation of liquid chromatography (LC) techniques, mass spectrometry becomes an even more powerful tool for metabolomics analysis. LC-MS is an analytical technique that utilizes the ability of liquid chromatography to utilize polarity to separate a mixture into its individual components, and a MS to detect mass information. Liquid chromatography has many approaches depending on the nature of the stationary phase, but perhaps the most well used type is Reverse Phase Liquid Chromatography (RPLC). RPLC is a broad term for a chromatographic column which uses a hydrophobic stationary phase. In this method, analyte elutes from the column in order of decreasing polarity. When liquid chromatography is used in addition to the mass analyzing properties of MS, one gets a technique that is highly sensitive, and has a high throughput. This combined technique is well used in metabolomic studies, as often crude plant extracts are analyzed to investigate their entire complement of metabolites. Considering advances in technology, as well as advances that may come in the future, it is an exciting time to study in the field of metabolomics. Minimizing risk becomes a more valuable objective than ever with the increase in sensitivity of analytical machines and software. Small, seemingly insignificant actions or choices during development of plant tissues, harvest, and particularly extraction could cause inconsistencies between samples that are difficult to reproduce.

Looking into the metabolism of a species or genotype is an excellent way to shed light on the inner workings of the organism at a precise moment in time. The analysis of the metabolome of the two arabidopsis tRNA-IPT gene mutants throughout the life cycle will show what, if anything, the reduction of cZ has done to the metabolism of the plants, and determine the masses of some metabolites that have had their levels altered significantly.

1.4.1 Data Analysis: Metabolite Databases

Analysis of mass spectral data has come a long way since the days of physical peak picking on large printouts of spectra. Nowadays, results may be uploaded to a cloud-based server, and analyzed nearly automatically, providing the user with a list of the most significant metabolite features. From there, acquiring MS-MS data can result in the elucidation of metabolite structures, and the production of spectra to be considered later. The challenge of converting experimentally detected MS signals into metabolite identities represents a key step that has been a preoccupation for several years. This has helped to justify the need for comprehensive metabolite databases (Bundy, Davey, & Viant, 2009). The METLIN (METabolite LINk) metabolite database (http://metlin.scripps.edu) is one of these online databases with which MS/MS spectra (which have already been positively identified and uploaded to the database) can be used to match with MS/MS spectra of potential metabolites. Determining chemical structure is often limited by the amount of information obtained during analysis, and the skill and experience of the researcher themselves. Typically, the more high-quality data that is acquired about a specific feature, the more accurately and quickly an identification can be performed.

1.4.2 XCMS

For untargeted metabolomics data there are a few platforms available for data processing. XCMS Online (*X* chromatography mass spectrometry; https://xcmsonline.scripps.edu) is a cloud-based server that is widely used for targeted and untargeted metabolomics studies because it is constantly updated, free to use, open source, capable of high throughput batch processing, and thoroughly cited (Q. Liu et al., 2012; Navarro-Reig, Jaumot, García-Reiriz, & Tauler, 2015; Sun et al., 2010). With any data processing software, there are five to six steps to process the raw LC-MS data. First, peaks must be identified and filtered in the total ion chromatogram. Second, peaks must be matched across samples (i.e. control vs treatment). Third, retention time may need to be corrected, and peaks may be realigned with the corrected data. Fourth, missing peaks may be filled in based on comparison between replicates, and fifth, appropriate statistical analyses are normally performed on the results. The sixth step is visualizing significant peaks, which can be done natively with XCMS Online, or XCMS can export a peak table that can be analyzed by other software.

1.5 Purpose

The aim of this project was to set the groundwork for understanding the significance of cZ in *Arabidopsis* growth and development through two methods: phenotyping to discern visible differences between cZ impaired mutants and wild type, and metabolomics to tease apart the differences that cannot be observed at the macro level.

Chapter 2: Materials and Methods

2.1 Plant Material

Plant material that was used is described in Table 1. All materials were obtained from the Arabidopsis Biological Resource Center (ABRC; https://abrc.osu.edu/). A wild-type control was grown in identical conditions alongside two tRNA-IPT silenced mutants, AtIPT2 and AtIPT9. The AtIPT2 has two exonic t-DNA insertions, while AtIPT9 has one insertion to silence one of the two genes responsible for *cis*-cytokinin production (K. Miyawaki et al., 2006).

Table 1: Genotypes of *Arabidopsis thaliana* used in this project.

Line	Description	Strain	Source
CS1092	Wild type	Columbia	ABRC
SALK_042050C	IPT2 gene silenced	Columbia	ABRC
CS313717	IPT9 gene silenced	Columbia	ABRC

2.2 Planting and Germination

Approximately 25 *Arabidopsis* seeds were sprinkled on top of moistened soil (Sungro Horticulture, Canada) in a 9.5cm x 9.5cm x 12cm plastic pot. Pots were then covered to block light and placed in a fridge at 4°C for 48 hours. For metabolite/CK analysis the pots were placed in a growth chamber (Conviron PGR15 growth chamber (Winnipeg, Manitoba, Canada) maintained at 23°C over a 16 h light: 8 h dark photoperiod, utilizing fluorescent lamps (F72T8/HO/TL841, Philips Electronics Ltd., Markham, Ont.) as a light source. Plants for biometrical analysis were grown in a greenhouse. Both sets of pots were covered with transparent plastic wrap. Nine small holes were punctured in the plastic wrap of each pot for gas exchange. Plastic wrap was removed for 5 minutes each day until the first seedlings appeared, when it was then removed permanently. Seedlings were plucked with tweezers until only a single, central plant was left. Any further seedlings that appeared were subsequently removed. Pots were then spread about 8 cm apart.

2.3 Biometrical Analysis

Multiple measurements were taken every three days during the growth of 8 wild-type, 8 AtIPT2, and 8 AtIPT9 plants. These measurements included the date planted, date of germination, date of first flower emergence, growth stage, rosette diameter, number of rosette leaves, number of shoots, number of primary, secondary, and tertiary branches, and total height of the plant at the highest point. A few measurements were taken at the end of the growth cycle to avoid impacting the growth of young plants. These measurements included above-ground fresh weight, above-ground dry weight, silique length (average of 4) and silique mass (average of 4).

2.4 Chlorophyll Extraction

A chlorophyll extraction was performed as outlined by Hiscox & Israelstam (1979) on dedicated plants grown alongside the other biometrical analysis plants to avoid influencing the measurements of the others. 100 mg of basal leaf tissue was harvested from 8 replicates of each line. The leaf tissue was cut into small pieces with scissors and placed in a vial containing 7 mL dimethylsulfoxide (DMSO), then placed in a water bath at 65°C for 20 minutes. 3 mL of DMSO were added to the extract to bring the total volume to 10 mL. 1 mL of extract was pipetted into a 1 mL cuvette, and placed into a Thermo Scientific Genesys 20 spectrophotometer. Light absorption values were tested at 645 nm and 663 nm against a DMSO blank. Using absorption values, the concentrations of chlorophyll A & B, total chlorophyll, and carotenoids were calculated using the formula in Hiscox & Israelstam (1979).

2.5 Phytohormone Profiling

2.5.1 Tissue Sampling

Plant tissues from all genotypes were harvested from dedicated plants at four growth stages, with four replications at each stage as documented in Boyes, 2001:

1. Emergence of first leaves (1.04) - entire plant
2. First flower opens (6.00) - basal leaf tissue
3. Ripening of silique seed pods (8.00, only green siliques were selected) – siliques
4. Mature seed (9.70) - only dry seeds

Tissue samples with roots were rinsed with ice cold water if necessary to remove any soil. 100 mg of tissue were collected and placed in 2 mL Eppendorf tubes, and placed in a freezer at -80°C until extraction.

2.5.2 Cytokinin Extraction

CK extraction and purification was carried out as described in Quesnelle & Emery (2007), and as modified by Farrow & Emery (2012). Methanol (CH_3OH; HPLC grade), acetonitrile (CH_3CN; HPLC grade), formic acid (HCO_2H; 88%), ammonium hydroxide (NH_4OH; 28%), and acetic acid (CH_3CO_2H; 97%) were obtained from Fisher Scientific Company (Ottawa, ON, Canada). Ultra-pure water was from a Millipore system (H_2O; Etobicoke, ON, Canada). A zirconium oxide grinding bead (ZnO_2, Comeau Technique Ltd., Vandreuil-Dorion Canada) was added to the Eppendorf tubes containing leaf tissue. Two beads were added to silique and mature seed samples to grind the tissue more effectively. 1 mL of -20°C Bieleski No. 2 extraction buffer (CH_3OH : H_2O : HCO_2H [15 : 4 : 1, v/v/v] was added, along with 10 ng of each of the following deuterated internal standards: ([$^2H_4$]ABA, [$^2H_7$]BA, [$^2H_7$]BAR, [$^2H_5$]ZOG, [$^2H_7$]DHZOG, [$^2H_5$]ZROG, [$^2H_7$]DHZROG, [$^2H_6$]iP7G, [$^2H_5$]Z9G, [$^2H_5$]2MeSZ, [$^2H_6$]2MeSiP, [$^2H_5$]2MeSZR, [$^2H_6$]2MeSiPR, [$^2H_6$]iPR, [$^2H_5$]ZR, [$^2H_3$]DHZR, [$^2H_6$]iP, [$^2H_3$]DHZ, [$^2H_5$]Z, [$^2H_6$]iPRMP, [$^2H_6$]ZRMP, [$^2H_3$]DHZRMP) (OlChemIm Ltd., Olomouc, Czech Republic). Labeled cZ CKs were not commercially available at the time of the extraction thus, analysis of cZ-types was evaluated relative to the recovery of labeled tZ-types and retention time of unlabeled cZ CKs.

Samples were homogenized in 2mL tubes using a Retsch MM 300 ball mill for 5 minutes at 25 Hz frequency and then stored overnight at -20°C for passive extraction. Tubes were subsequently spun down at 10 000 rpm for 10 min, and the supernatant transferred to a fresh 2 mL tube and dried at ambient temperature under vacuum

(Speed Vac Model SPD111V; Thermo Scientific, Ottawa, Canada). Further purification was performed by re-dissolving residues in 1 mL of 1 M formic acid, and running the solvent through a mixed mode, reverse-phase, cation-exchange SPE cartridge (IRIS MCX 200 mg/6.0 mL, Canadian Life Sciences, Peterborough, Canada) as previously described by Quesnelle & Emery (2007) with modifications Farrow & Emery (2012). SPE cartridges were activated with 5 mL analytical grade methanol, followed by 1 M formic acid. Samples were loaded, and fractions eluted by their polarity. ABA was eluted first with methanol, followed by the nucleotide fraction (CKNTs) using 0.35 M ammonium hydroxide. Free bases (CKFBs) and ribosides (CKRs) were then eluted with 0.35 M ammonium hydroxide in 60% v/v methanol. All fractions were dried at 35°C in the Speed Vac and then stored at -20°C. CKNTs were degraded into ribosides with 3 units of bacterial alkaline phosphatase (New England Biolabs Ltd., Whitby, ON, Canada) in 1 mL 0.1 M ethanolamine for 12 hours at 37°C. Resulting CK ribosides were dried in the Speed Vac at ambient temperature. This nucleotide detection method potentially reflects a pooled contribution of mono, di- or triphosphates in that the isopentenyl or hydroxylated moiety can be transferred to AMP (adenine monophosphate), ADP (adenine diphosphate) or ATP (adenine triphosphate). Residues were reconstituted in 1.5 mL of Milli-Q water and passed through a reverse-phase C18 column for purification (C-18 Octadecyl 14% 500 mg/6.0 mL, Canadian Life Sciences, Peterborough, Canada). Columns were activated with 3mL methanol and equilibrated with 3 mL of Milli-Q water twice. The columns were loaded with samples and run through under vacuum. Columns were washed with 3 mL Milli-Q. Derivatized CKNTs were eluted with 1.25 mL methanol via gravity. Sample eluates were dried at ambient temperature in a Speed Vac. and stored at -20°C if necessary. Samples were then re-dissolved, spun down at 10000 rpm for 10 min, and the supernatant transferred into 2 mL glass vials. The solvent used to re-dissolve the samples depended on which fraction was in the tube, CKFBs, CKRs, and CKNTs were dissolved in 0.08% v/v acetic acid in 5% v/v ACN, and ABA was dissolved in 5% v/v methanol in 0.08% v/v acetic acid.

Leaf tissue was analyzed for CK using high performance liquid chromatography – positive electrospray ionization – tandem mass spectrometry (HPLC-(+ESI)-MS/MS) methods and multiple reaction monitoring (MRM) channels, specific for each analyte, were carried out as described in Farrow & Emery (2012). Samples were analyzed and quantified using a Shimadzu LC (Kyoto, Japan) connected to a 5500 QTrap triple quadrupole mass spectrometer (Sciex Applied Biosystem, Concord, ON, Canada) with a turbo V-spray ionization source. Mature seed was analyzed with a Thermo Q-Exactive Orbitrap mass spectrometer coupled to a Thermo Dionex UltiMate 3000 HPLC. A 20 µL sample was injected onto a Halo 2.7µm C18 column (50 mm × 2.1 mm; Canadian Life Science) and all samples were analyzed in positive-ion mode. All hormone fractions were eluted with component A: H_2O with 0.08% CH_3CO_2H and component B: CH_3CN with 0.08% CH_3CO_2H, at a flow rate of 0.4 mL min^{-1}. The CK fractions were eluted with a multi-step gradient. Starting conditions were 5% B increasing linearly to 10% B over 2 min followed by an increase to 95% B over 6.5 min; 95% B was held constant for 1.5 min before returning to starting conditions for 5 min.

2.5.3 Cytokinin Quantification

Leaf and silique tissue data were analyzed with Analyst 1.5.1 software (AB SCIEX, Concord, ON, Canada). CKs were identified based on their MRM precursor-fragment ion transitions and retention times. Concentrations were determined according to isotope dilution analysis based on direct comparison of the endogenous analyte peak area to that of the recovered internal standard. Seed tissue data were analyzed with Xcalibur 3.1 (Thermo Scientific, Rockwood, TN). CKs were again identified based on their MRM channels and retention times. Concentrations were determined using the same method, being determined according to isotope dilution analysis based on comparison of the endogenous analyte peak area and the peak area of the recovered internal standard.

2.6 Statistical Analysis

Statistical analysis of cytokinin levels and growth data was performed with Statistica 8 software. Measurements were compared within each growth stage with an ANOVA, followed by a Duncan post-hoc test to determine significance between mutants and WT. Analysis of metabolite significance was determined through an unpaired t-test automatically performed by XCMS Online when LC-MS data is analyzed. Only metabolites with a p-value < 0.05 were considered for further analysis.

2.7 Metabolite Analysis

2.7.1 Metabolite Extraction

Plant tissues were sampled at the same growth stages and in the same manner as in the phytohormone profiling method. Tissues were placed in 2 mL Eppendorf tubes with a grinding bead (two for silique and mature seed samples), immediately frozen in liquid nitrogen, and stored at -80°C if extraction was to be performed at a later date. Samples were frozen again in liquid nitrogen just prior to loading into the ball mill, four at a time. Tubes were shaken for one minute at 25 Hz. 1. The powder was suspended in 1 mL of ice cooled 80% MeOH/20% water v/v and sonicated for 15 minutes. Tubes were spun down at 10 000 rpm for 10 minutes. 700 µL of sample supernatant was transferred to 0.2 µM PVDF centrifuge filters with 2mL receiver tubes and spun down at 4000 rpm for 3 minutes. Filtered extracts were dried down at ambient temperature in the Speed Vac. Residues were re-dissolved in 400 µL 50% MeOH/Water and spun down again at 10000 rpm. 200µL of supernatant was transferred to a 400 µL autosampler insert inside a 2 mL glass vial with septa cap. 10 µL of $[^2H_7]$BA (*m/z* 233.1527) standard was added to use as a lock mass and monitor retention times across samples.

2.7.2 Full Scan Analysis

Initial metabolite full-scan analysis was carried out as described by (Renaud, Sabourin, Topp, & Sumarah (2017), with some modifications to suit available equipment. MS data were acquired with a Thermo Q-Exactive Orbitrap mass spectrometer (Rockford, Illinois) coupled to a Thermo Dionex UltiMate 3000 HPLC

(Rockford, Illinois). A volume of 25µL of each sample was injected onto a Halo 2.7µm C18 column (50 mm × 2.1 mm; Canadian Life Science) using a flow rate of 0.3 mL min−1 with a mobile phase of LC−MS grade water (Milli-Q) with 0.1% formic acid (A) and LC−MS grade acetonitrile (Fisher) also with 0.1% formic acid (B). Mobile phase B was held at 0% for 30 s, before increasing to 100% over 3 min. Solvent B was then held at 100% for 2 min before returning to 0% over 4 minutes, to allow pressure to stabilize. The following conditions were used for heated electrospray ionization (HESI): capillary temperature, 250 °C; sheath gas 30 arbitrary units; auxiliary gas, 8 units; probe heater temperature, 450 °C; S-Lens RF level, 60%; and capillary voltage, 3.9 kV. For HRMS, sample acquisition each sample was analyzed in positive ion mode focusing in a mass range of *m/z* 100−600, and were acquired at 140k resolution, automatic gain control (AGC) target of 3×10^6, and maximum injection time (IT) of 524 ms.

2.7.3 Metabolite Selection

Data files (as Thermo.RAW) were directly uploaded to XCMS Online (https://xcmsonline.scripps.edu) in order find significant differences between the metabolite profiles of the AtIPT mutants and the wild-type, and identify metabolite features (unknown metabolites). Parameters for the analysis were selected as outlined by Chen et al., 2017, with modifications to tailor the method to the HPLC in lab. Metabolite detection was completed with the centWave method and a ppm tolerance of 1 (a match provided automatically by XCMS must not have a mass accuracy value <1ppm). Mass Accuracy was calculated as follows: = $1e^6$ * (observed mass – exact mass)/ exact mass. The pre-filter was set to six scans with a minimum 5,000 intensity, the signal to noise threshold was 5 and noise was set to 1×10^6 for use in positive mode. A retention time correction was conducted using the obiwarp method; the grouping included features present in at least 25% of all samples, the allowable retention time deviation was 10 s, and the *m/z* width was set to 0.015. The 'fillPeaks' function with default settings and remaining zeros was imputed with two-thirds the minimum value on a per mass basis. Using the XCMS generated results table, a list the most significant features (*p* value <0.05) was drafted and retained for later PRM analysis to provide MS/MS spectra for these potential features. Prior to PRM analysis the peak list was further filtered to select high quality peaks. Criteria for feature selection included: average retention time of greater than or equal to 1.5 min to less than or equal to 6 min to avoid solvent fronts and tails during the pressure rebound of the HPLC, a fold change greater than 1, a visual representation of the peak in XCMS was used to check peak shape and intensity. A further verification step was performed in Xcalibur using the truncated list. The *m/z* values of the high-quality peaks were cross-referenced between all sample replicates containing a specific peak to (i) determine which sample contained the highest peak intensity of the *m/z* in question, and (ii) verify the peak could be found in both XCMS and Xcalibur.

2.7.4 PRM Analysis

Parallel Reaction Monitoring (PRM) mode analysis of the selected peaks was performed as per Renaud et al. (2017). The peaks selected for PRM mode during the selection process were used to create four methods with approximately 10-12 features each to avoid potential over-saturation of the instrument during acquisition. During preliminary scans, the Normalized Collision Energy (NCE) was increased incrementally from 30 to 50. This provided satisfactory fragmentation in the majority of the selected features for use in online metabolite databases to determine possible identities.

2.7.5 Metabolite Identification

Utilizing the spectra acquired in PRM mode, a peak list for each metabolite precursor ion and its product ion fragments was drafted, and possible formulas were assigned to the peaks with Xcalibur. The constraints of the formula prediction were as follows: Carbon: 1-50, Nitrogen 0 – 8, Hydrogen 1-100, Oxygen 0 – 10, Sulfur 0-2. Predicted formulas were then used to calculate theoretical mass and the mass accuracy of the predicted formula. Only mass accuracy less than an absolute value of 5ppm was accepted. The relative intensities of the product ion peaks were used to determine which were useful for use in metabolite database searches. METLIN was used as a quick search with only the *m/z* of the unfragmented feature, specified a positive ion (or simply neutral if using a calculated neutral mass), with [M+H], [M+Na], [M+ACN] adducts specified. METLIN provided some suggestions for an identity, and occasionally simulated MS/MS spectra of the matches to use to confirm identity by cross referencing with the product ion *m/z* values and/or predicted chemical formulas. The MassBank(https://massbank.eu) database was also used alongside METLIN to cross reference and identify peaks. *m/z* values and relative intensities of product ions of a feature were entered and the site returned a list of MS-MS spectra matches, which were used to cross reference with the corresponding relative intensity peak list and literature about the metabolite and its possible role in *Arabidopsis.*

Chapter 3: Results and Discussion

3.1 General Overview

Generally, it is thought that cis-CKs are relatively inactive compared to their transCK counterparts (Hluska, 2017). However, through analysis of both the phenotype and metabolome, this research tested the hypothesis that *cis*-CKs play a biologically significant role in *Arabidopsis thaliana,* and influence growth and metabolism of the plant. Mutant plants often express a unique visible phenotype, although that is not always the case. For example, double mutants from any possible combination of AtIPT 1, 3, 5 and 7 showed no visible phenotype; however when triple, quadruple, and quintuple mutants were grown, aberrant phenotypes began to appear as the plant aged; whereby plants had fewer rosette leaves, thin inflorescence stems, and greater lateral root growth (K. Miyawaki et al., 2006). Additionally, cytokinin deficiency created by overexpressing CKX genes in *Arabidopsis* resulted in diminished activity of the vegetative and floral shoot apical meristems and leaf primordia, indicating an absolute requirement for the hormone (Werner et al., 2003). In regard to AtIPT2 and AtIPT9 *cis*-CK suppressed mutants, there are only a few documented phenotypic differences. All that is known is that they may show stunted root growth and chlorotic leaves as a result of the lowered *cis*-CK levels (K. Miyawaki et al., 2006). Furthermore, *trans*-CK suppressed mutants have been shown to possess greater cell membrane stability and exogenous Abscisic Acid (ABA) hypersensitivity, even though it caused a downregulation in ABA biosynthetic genes, suggesting that mutual regulation mechanisms exist between CK and ABA metabolism (Nishiyama et al., 2011). Curiously, a lower *trans*-CK level was shown to increase primary root growth (Werner et al., 2003). This contrasts with the low *cis*-CK situation which suppresses primary root growth, and promotes lateral growth (K. Miyawaki et al., 2006). This suggests at least one difference in the mechanism of *cis* and *trans*-CK that can be demonstrated phenotypically by more closely documenting detailed differences in phenotype at key growth stages.

Sometimes visible differences in phenotype are not presented nor immediately apparent, and may even be overlooked if they are subtle, microscopic or even sub-cellular. One must dig deeper to find out if there is impact at the molecular level. Studying the metabolites that may differ between a WT and mutant is an excellent way to accomplish this, and can even shed light as to what the role of a particular gene or metabolite plays in a plant's metabolism by working backward from the metabolite identities. Even if a clear phenotype is present, it is still useful to evaluate the effects on metabolism, to more completely understand the metabolism of the plant.

In this thesis, I studied the effects of *cis-CK* suppression on the metabolism of *Arabidopsis* throughout its growth cycle via analysis of the effects of AtIPT2 and AtIPT9 gene silencing. The mutations of these genes were designed to disrupt the CK production via the tRNA-degradation pathway by restricting the production of tRNA-isopentenyltransferase (KEGG enzyme EC 2.5.1.75) as shown in Figure 1. Since AtIPT2 and AtIPT9 are potentially redundant and part of a bigger IPT gene family containing IPT 1-8 (K. Miyawaki et al., 2006), a careful evaluation of the impact of AtIPT2 and AtIPT9 gene silencing have directly on CK metabolites is necessary to understand if those genes, by themselves, can significantly alter the endogenous CK profile.

3.2 Cytokinin Concentrations

The tRNA-degradation pathway is interrupted in the mutants by the silencing of AtIPT2 & AtIPT9. If this pathway is impaired, it should hinder the production of cZ as well as 2MeS-CK, resulting in decreased levels (Figure 1), depending on if, and where, the genes are normally active. Therefore, to check the efficacy of the mutants obtained from the ABRC that are designed to disrupt AtIPT2 and AtIPT9 by insertion, CKs were measured by LC-MS/MS. The relative levels of cZ shown in Figure 5, indicate that the AtIPT2 mutant accumulates lower total cZ-forms in the first leaves, as well as during silique formation. The AtIPT9 mutant showed reduced total *cis*-CK in first leaves as well. Interestingly, once silique development was tested, the levels cis-CK in AtIPT9 were greater than those of the WT plants. Although shown as statistically significant in a Duncan's post-hoc test, the cZ levels of AtIPT9 were only slightly higher by just approximately 6 pmol/gfwt (picomole per gram fresh weight). However, it could have also been a compensatory response of AtIPT2 in response to lower IPT9 activity. As of yet, there has not been a detailed study of expression levels of AtIPT2 and 9 across development and among tissues/organs. A possible explanation may lie in how the expression of the two AtIPT genes differs. Thus, there is a need for more targeted research into the expression of these AtIPT2 and AtIPT9 genes.

Total iP, shown in Figure 5, indicates that the relative levels at growth stages beyond 1.04 are very similar between WT and the mutants in all stages. This could be because *Arabidopsis* predominantly produces iP type cytokinins via the *de novo* pathway, rather than the tRNA pathway, thus mitigating the impact of the interruption of tRNA-IPT. This is in line with previous analysis of AtIPT 1 3 5 7 mutants, for which iP type cytokinins were greatly decreased when impaired via AtIPT 1 3 5 7 gene silencing (K. Miyawaki et al., 2006). In the case of growth stage 1.04, first leaves of the mutants accumulated significantly lower levels of iP-type cytokinins compared to the WT. It is possible that this is due to the tRNA-degradation pathway playing a more prominent role in the vegetative growth of young plants. In addition, the iP levels remained relatively consistent among lines within growth stages 6.0, 8.0, and mature seed (9.7), with the exception of first leaf tissue. However, levels in all lines differed greatly between growth stages, with seed tissue showing the greatest levels of iP. In first leaves WT had high iP levels, possibly due to both the *de novo* and tRNA-degradation pathways being active, resulting in higher levels initially.

Figure 5 shows relative levels of methylthiol (2MeS) cytokinins. 2MeS are poorly understood cytokinins (Kambhampati et al., 2017). They were found at varying concentrations throughout plant growth, and in similar quantities in both WT and mutants suggesting that 2MeS cytokinins may not play an impactful role in *Arabidopsis* development. That said, the levels in silique development and mature seed were higher in mutants relative to the other growth stages. The 2MeS levels in siliques of the mutants were statistically higher ($p < 0.05$) than those of WT, with AtIPT2 mutant having the highest concentration, and AtIPT9 higher than WT, but below AtIPT2. Again, the redundant roles of AtIPT2 & AtIPT9 may be the cause for the different levels of accumulation of 2MeS in mature seeds. The non-mutated genes may over-express to compensate for one homologue being silenced, resulting in similar levels in mature seeds. The higher levels in the siliques of the mutants are consistent with this.

ABA is a different class of hormone from the cytokinins, but the two groups are often co-associated in many plant physiological processes, such as flowering (Wang et al., 2011). ABA quantities are shown in Figure 5. In siliques of the AtIPT2 mutant ABA was suppressed, while AtIPT9 was not significantly different than both WT and AtIPT2. Metabolome data also uncovered ABA effects (discussed in section 3.4), providing further evidence that cis-CK impairment affects ABA production and/or signaling.

The suppressed cis-CK levels of AtIPT9 shown in Figure 5 surprisingly coincide with increased rosette diameter, greater fresh weight, and flowering. Meanwhile AtIPT2 had none of these deviations except for increased flowering; despite exhibiting greater cis-CK supression than AtIPT9. Additionally, siliques contained suppressed cis-CK levels, but no phenotype deviations manifested in silique tissue. It appears as though both IPT2 and IPT9 indeed affect CK profile since different CK types and quantities accumulate differently from WT, including particularly strong differences found in first leaves and siliques. Full CK profiles are shown in Table 3 in the Appendix.

3.3 Phenotyping

When a gene of significance is involved, some of the most apparent differences between controls and mutants will manifest in the phenotype. A different phenotype can be visually striking, such as stunted growth or leaf shape changes, or it may take closer observation to observe differences like chlorophyll and carotenoid content or changes of very small features that occur only in a short period of time. Both are meaningful, as a phenotype is a culmination of metabolic processes occurring within plant tissues. Therefore, a keen eye must be used when profiling phenotypes. To test the hypothesis that phenotypic deviations exist in the mutants, close observation throughout the growth cycle of the plants was used to track differences. Large physical changes like number of shoots, rosette and leaf sizes, plant height was recorded at 3-day intervals. Smaller changes in appearance such as trichome appearance were recorded with photography.

Measurements taken over a full growth cycle of the WT and mutants are shown in Figure 3. Overall, the most differences appeared in AtIPT9 which grew a larger rosette, had more flowers, retained flowers longer, had a greater fresh weight at maturity, and had more shoot-based leaves (Duncan, p-value < 0.05). However, AtIPT9 did have a shorter overall height compared to WT and AtIPT2, perhaps from the oversized growth of the rosette claiming more resources than the other cultivars. AtIPT9 had a greater above-ground dry mass than AtIPT2; however, this was not statistically different than the WT ($p > 0.05$). Silique size and mass were consistent among all cultivars, and the number of shoots was greater in both WT and AtIPT9 compared to

AtIPT2. In some cases, AtIPT2 also had significantly different phenotypic traits from the WT. AtIPT2 had fewer shoots and a lower dry mass on average than both WT and AtIPT9. This supports the hypothesis that AtIPT mutants manifest some phenotypic deviations, as AtIPT2 and AtIPT9 impairment positively affects growth of rosette and fresh weight, as well as increase flowering, implying a reduction in cis-CKs corresponds with changes in reproductive phenotype of both mutants. However, both mutants do not seem to share common phenotype changes in plant growth, despite both being cis-CK impaired.

Chlorophyll data shown in Figure 4 indicated no differences in chlorophyll A and B, or total chlorophyll. The mutants were suppressed in carotenoids however. This could be explained by the same pathway that resulted in the suppression of ABA in the mutants' siliques since ABA is synthesized through the carotenoid pathway (Ruiz-Sola & Rodríguez-Concepción, 2012). This is in line with previous research showing that CK has a role in delaying senescence and in turn retaining chlorophyll (Khan, Rozhon, & Poppenberger, 2013)

The growth of AtIPT9 exceeded both WT and AtIPT2 in regard to the size of leaves of the rosette, as well as number non-rosette leaves. In addition, AtIPT9 demonstrated stunted shoot elongation relative to WT throughout the growth cycle. AtIPT2 showed stunted shoot elongation initially, but upon plant maturation the shoots became the same length as WT. This agrees with previous observations that cytokinin deficient plants develop stunted shoots (Werner, Motyka, & Strnad, 2001).However these observations have only previously been seen in trans-CK mutants. Delayed initiation of flowering was observed in both mutants. Nevertheless, an increased number of flowers was observed in AtIPT9 and to a lesser extent AtIPT2. CK is known to promote flowering (D'Aloia et al., 2011) as well as the ratio of auxin to CK playing a role in flowering (Bernier, 1993). A peculiar but obvious observation came from the trichome development of the mutants. Trichomes were observed to grow noticeably longer, and denser in the mutants than those of the WT, as depicted in Figure 2. The increased trichome size coupled with increased flowering in the mutants is possibly linked, as cytokinins have been shown to influence both pathways, and genes that control trichome activation (An, Zhou, Yan, & Gan, 2011) are also positively associated with floral transition (Matías-hernández, Aguilar-jaramillo, Cigliano, Sanseverino, & Pelaz, 2016). Overall, it appears that a lack of cis-CK has strong effects on the phenotype of *Arabidopsis,* altering: trichome formation, flower development, carotenoid levels, and plant growth.

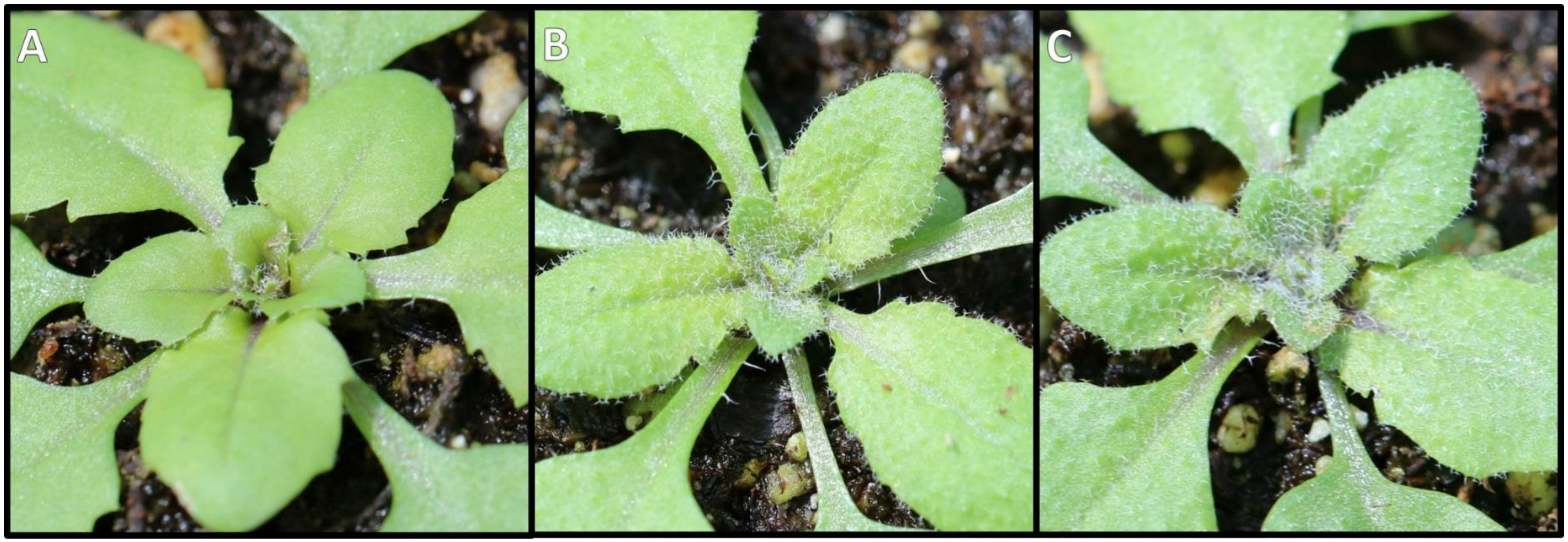

Figure 2: Example of trichomes in (A) WT, (B) AtIPT2, and (C) AtIPT9 plants.

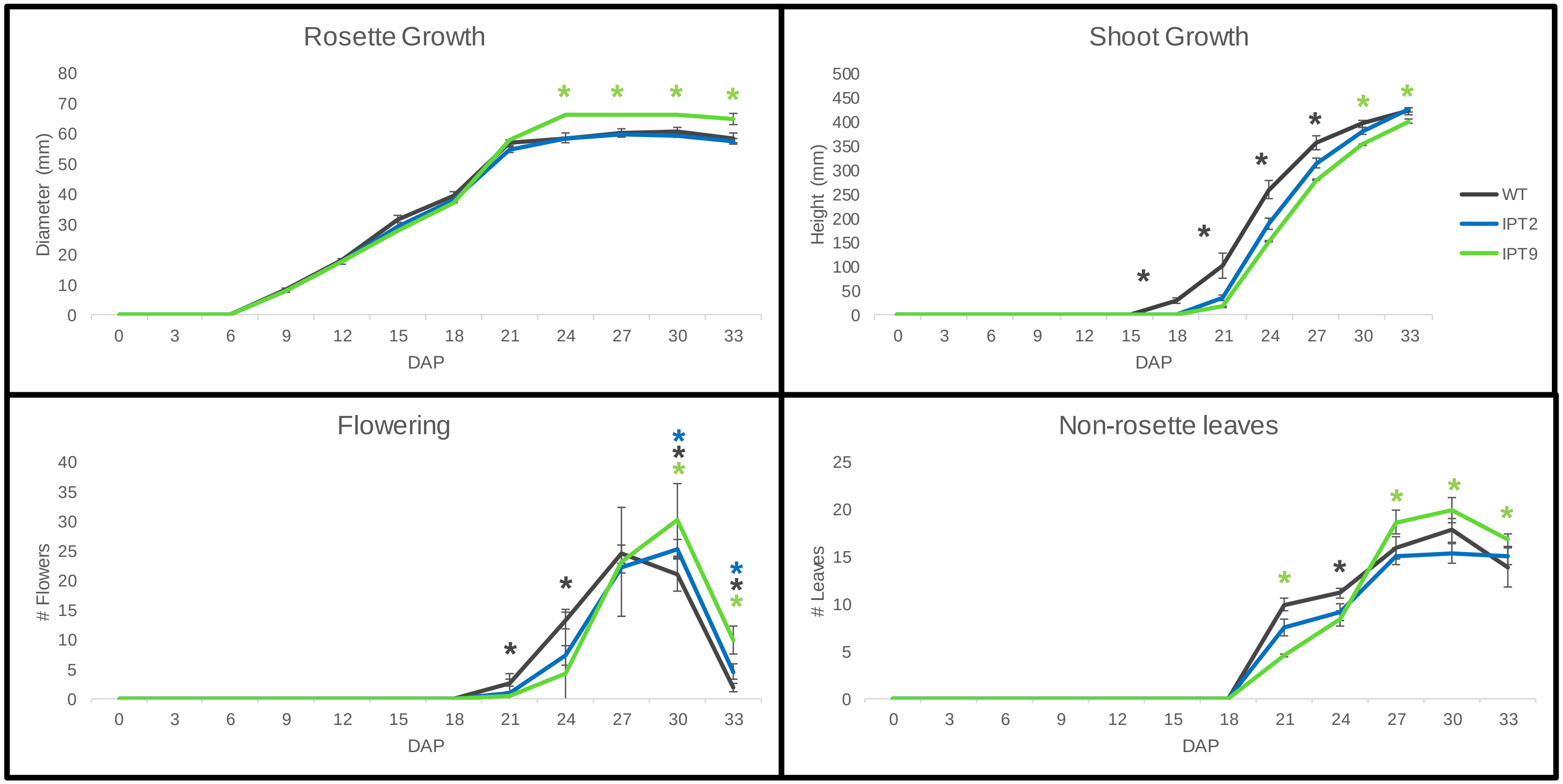

Figure 3: Measurements taken during growth of cultivars. Asterisk (*) symbolizes significance vs. other ecotypes with colour corresponding to ecotype. Multiple asterisks depict significance between more than one ecotype. X axis depicts time scale, measured by Days After Planting (DAP).

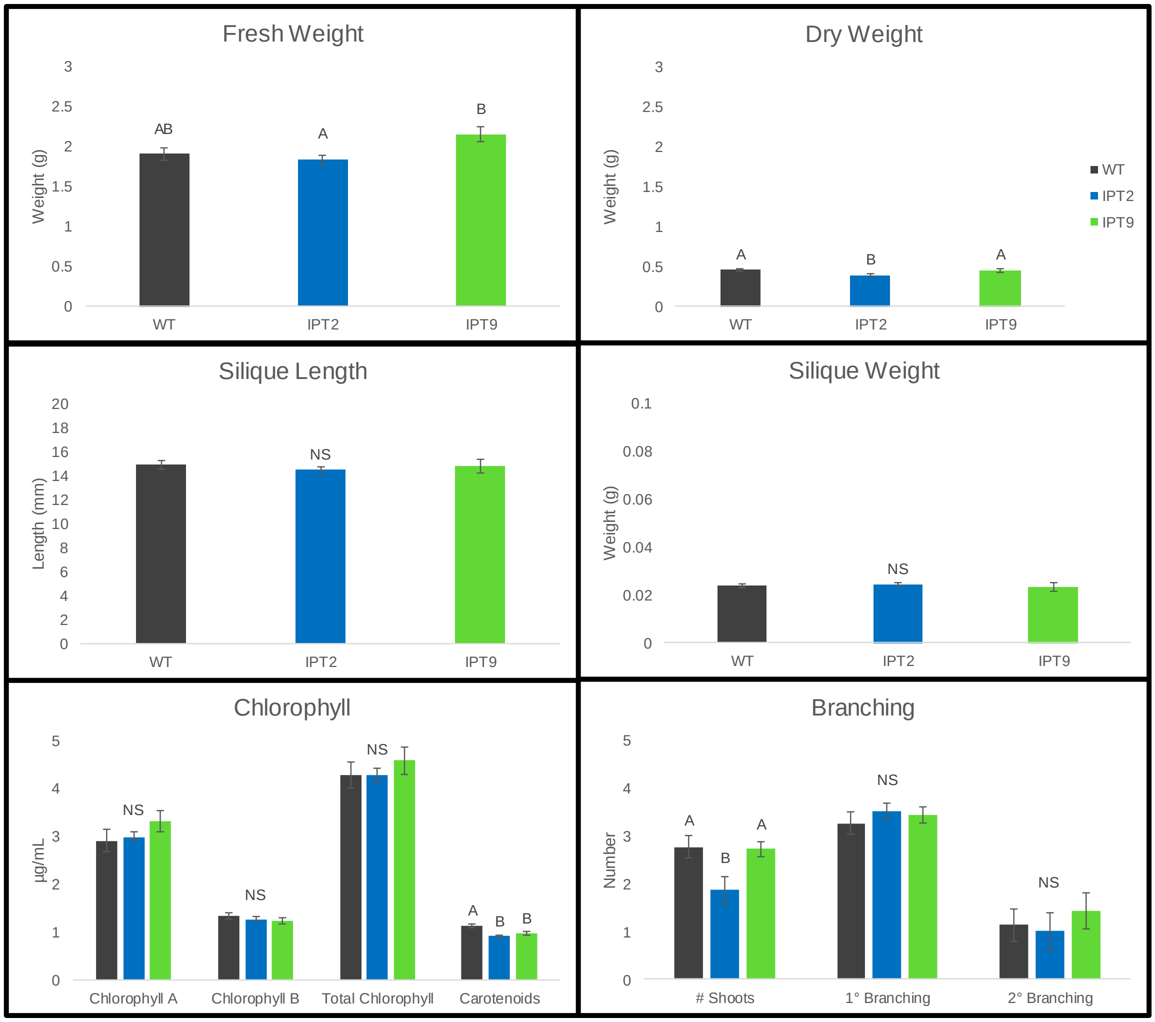

Figure 3: Post-mortem measurements taken at completion of growth cycle. Letters indicate significant values, identical letters indicate values are significant, but not from each other. NS indicates no significance.

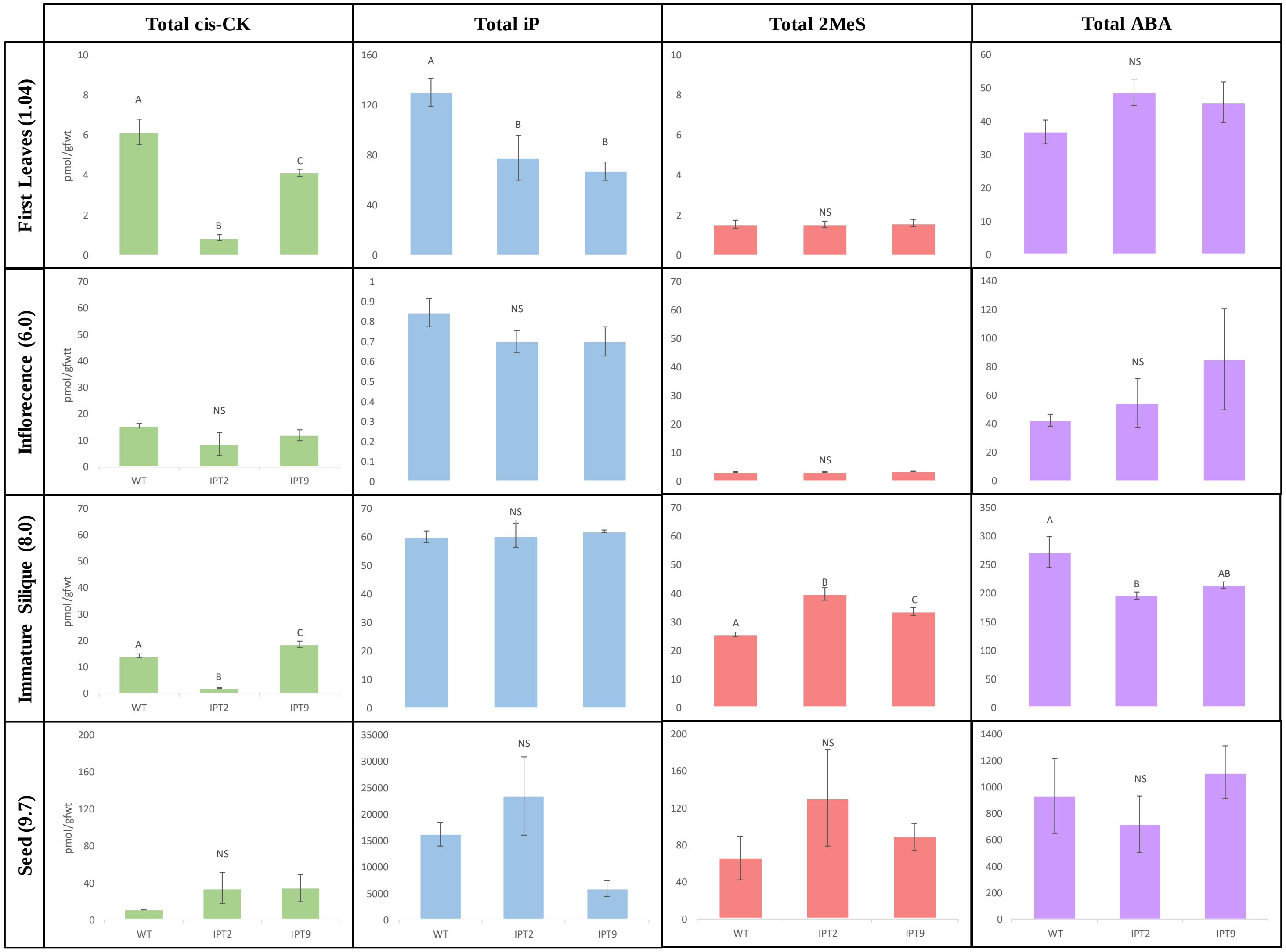

Figure 4: Total cis-cytokinin (cis-CK) type, isopentenyladenine (iP) type, and methylthiol type (2MeS) cytokinin levels, along with abscisic acid (ABA) levels at different growth stages of *Arabidopsis*. Letters indicate significant values, identical letters indicate values are significant ($p < 0.05$, n=4), but not from each other. NS indicates no significance.

3.4 Metabolite Analysis

In the previous sections (3.2 and 3.3) it was shown that both CK profiles and phenotypes were disrupted by mutations in AtIPT2 and AtIPT9. Phenotype differences were observed with CK metabolite changes in the case of vegetative growth, but not in siliques. However, CK levels and phenotypes not corresponding does not rule out meaningful impact by cis-CK. Many metabolic processes occur between transcription and expression of the phenotype. In some cases, some major changes never manifest into a visible phenotype. Therefore, this research investigated at the metabolome level to test the hypothesis that the cis-CK impaired mutants AtIPT2 and AtIPT9 would exhibit changes in metabolism vs the WT that do not result in obvious phenotype deviations.

Investigating differences in AtiPT2 and AtIPT9 metabolite levels is crucial to further the understanding of how these mutants work, particularly when *cis-CK* levels are affected. The interruption of the tRNA-degradation pathway should alter the metabolite profile in a way that reflects the metabolism that is under the influence of *cis-CK*. This is the basis that was used to test the changes through acquisition of LC-MS/MS data from: the same four growth stages as CK analysis, selection of significant metabolites with XCMS, and matching with known metabolites in databases such as METLIN and MassBank.

A total of 36 significant (t-test, $p<0.05$) metabolite features that differ in intensity and/or presence/absence vs the WT were noted in Table 2, with a number of features showing possible matches in the METLIN and MassBank metabolite databases. A “feature” in this study is defined as a bundle of data values (m/z, RT, p-value, foldchange, etc.) corresponding to an ion peak within mass spectra. While it is not possible to make definitive metabolite identifications without a known standard, tentative database matches can be made. Variations from database *m/*z values and chemical formulas can arise. Mass accuracy of predicted formulas, and variation in sensitivity of the MS instrument throughout an analysis can cause small errors in measurement that deviate from literature and database values. However, the metabolite features described in this thesis were best-fit matches with the databases, and contain small deviations from the database values, and are supported by references that have previous demonstrated their presence in *Arabidopsis,* or their role in plant metabolism. 30 of these metabolites were unique *m/z* values and the other 6 were duplicates across growth stages, or occurred in both mutants. AtIPT2 had 11 significant features, with one common *m/z* occurring in the inflorescence and silique growth stages. AtIPT9 had 25 *m/z* values different than WT. Four of the features were common with those observed for AtIPT2. The number of features identified compares well with other exploratory metabolite studies in which a mutant approach was used. (Fukushima et al., 2014; Wen et al., 2015). In the following discussion, metabolite features that are common to both mutants will be considered first, followed by features that change in only one mutant. From there evidence for identification, biological relevance, and any known ties to CK and hormones will be discussed.

Table 2: Metabolite features found at different stages of *Arabidopsis* development.

Genotype	Growth Stage	Observed (*m/z*)	Ion	Predicted Formula	Theoretical Mass (*m/z*)	Mass Accuracy (ppm)	Product Ions	NCE	UP/DOWN	Fold	*p*-value	Proposed Compound	Reference
	FIRST LEAVES (1.04)	158.0811	$[M+H]^+$	$C_7H_{11}O_3N$	158.0812	-0.7442	116, 112, 110, 93, 70, 69	50	DOWN	1.7	0.01876	N-acetylproline	METLIN ID: 43543
		188.1103	$[M+H]^+$	$C_9H_{17}ONS$	188.1104	-0.3097	188, 124, 107, 82, 79, 65	50	DOWN	1.7	0.03507	-	
		195.1015	$[M+H]^+$	$C_{11}H_{14}O_3$	195.1016	-0.3681	138, 107, 163, 153	50	DOWN	1.1	0.00409	-	
		227.1276	$[M+H]^+$	$C_{12}H_{18}O_4$	227.1278	-0.6870	181, 167, 100, 86	50	DOWN	2.5	0.00044	12-hydroxy jasmonate	METLIN ID: 36075
	INFLORESCENCE (6.0)	207.0652	$[M+H]^+$	$C_{11}H_{10}O_4$	207.0652	0.0464	192, 175, 157, 147, 119, 91	50	DOWN	1.5	0.03833	Vinyl caffeate	METLIN ID: 86482
IPT 2													
	SILIQUE (8.0)	207.0652	$[M+H]^+$	$C_{11}H_{10}O_4$	207.0652	0.0464	192, 175, 157, 147, 119, 91	50	UP	2.7	0.00095	Vinyl caffeate	METLIN ID: 86482
	SEEDS (9.0)	114.0372	$[M+H]^+$	C_5H_7NS	114.0372	-0.0644	114,72	50	UP	1.4	0.00794	4-Isothiocyanato-1-butene	METLIN ID: 89578
		138.0550	$[M+H]^+$	$C_7H_7O_2N$	138.0550	0.4866	96	50	UP	2.5	0.00542	-	
		157.0495	$[M+H]^+$	$C_7H_8O_4$	157.0495	0.0145	157, 142, 130, 129, 116	50	UP	1.8	0.00334	-	
		220.0824	$[M+H]^+$	$C_9H_{17}ONS_2$	220.0824	-0.1640	156, 124, 123, 97, 95, 79, 69, 55	50	UP	2.0	0.00001	1-Isothiocyanato-7-(methylsulfinyl)-heptane	MassBank Record: PR101035
	FIRST LEAVES (1.04)	123.0804	$[M+H]^+$	$C_8H_{10}O$	123.0804	-0.4428	95, 81	50	DOWN	1.5	0.02200	-	
		139.0753	$[M+H]^+$	$C_8H_{10}O_2$	139.0754	-0.2596	97, 56	50	DOWN	1.2	0.00027	-	
		158.0811	$[M+H]^+$	$C_7H_{11}O_3N$	158.0812	-0.7390	116, 112, 110, 93, 70, 69	50	DOWN	1.8	0.00444	N-acetylproline	METLIN ID: 43543
		220.1177	$[M+H]^+$	$C_9H_{17}O_5N$	220.1179	-0.9325	156, 123, 114, 97, 69. 65, 55	50	DOWN	1.3	0.03263	1-Isothiocyanato-7-(methylsulfinyl)-heptane	MassBank Record: PR101035
		290.1595	$[M+H]^+$	$C_{12}H_{17}ON_8$	290.1598	-1.1655	126, 84	50	DOWN	1.1	0.03484	-	
	INFLORESCENCE (6.0)	114.0372	$[M+H]^+$	C_5H_7NS	114.0372	-0.0644	114, 72	50	DOWN	1.8	0.04357	4-Isothiocyanato-1-butene	METLIN ID: 89578
		178.0354	$[M+H]^+$	$C_6H_{11}ONS_2$	178.0355	-0.2625	119, 114, 72, 55	50	DOWN	1.8	0.04205	Sulforphane	MassBank Record: PR100442
		180.0311	$[M+H]^+$	$C_3H_7O_3N_4S$	180.0312	-0.5089	121, 119, 116, 114, 74, 72, 55	50	DOWN	1.8	0.04266	-	
		205.0971	$[M+H]^+$	$C_{11}H_{12}O_2N_2$	205.0972	-0.0923	124, 106	50	UP	1.9	0.01004	L-Tryptophan	METLIN ID: 268269
	SILIQUE (8.0)	160.0756	$[M+H]^+$	$C_{10}H_9ON$	160.0757	-0.5093	145, 117, 129, 128, 96	50	UP	1.8	0.01871	Indole-3-acetaldehyde	METLIN ID: 6068
		239.0880	$[M+H]^+$	$C_8H_{18}O_2N_2S_2$	239.0882	-1.0384	147, 119, 114, 105, 95, 91, 72, 62	50	UP	1.9	0.03487	-	
IPT 9													
	SEEDS (9.0)	108.0807	$[M+H]^+$	C_7H_9N	108.0808	-0.4562	93, 91, 80	50	UP	2.5	0.00767	-	
		110.0964	$[M+H]^+$	$C_7H_{11}N$	110.0964	-0.1821	93,69	50	UP	2.6	0.00860	-	
		122.0964	$[M+H]^+$	$C_8H_{11}N$	122.0964	-0.2994	120	50	UP	2.3	0.00975	-	
		124.0393	$[M+H]^+$	$C_6H_5O_2N$	124.0393	0.3375	107, 82, 79	50	UP	2.6	0.00195	Nicotinic acid	METLIN ID: 266640
		130.0651	$[M+H]^+$	C_9H_7N	130.0651	0.1033	-	50	UP	1.8	0.03833	Quinoline	METLIN ID: 66396
		135.0997	$[M+H]^+$	$C_4H_{12}O_2N_3$	135.1002	-3.6416	107, 93, 91, 79	50	UP	2.4	0.00940	-	
		137.1154	$[M+H]^+$	$C_4H_{14}O_2N_3$	137.1159	-3.4292	122, 109, 95, 81, 67	50	UP	2.1	0.00146	-	
		176.0562	$[M+H]^+$	$C_7H_{13}NS_2$	176.0562	-0.1380	96, 92, 80, 79, 69, 55	50	UP	2.9	0.00148	1-Isothiocyanato-5-(methylthio)-pentane	METLIN ID: 87781
		207.0652	$[M+H]^+$	$C_{11}H_{10}O_4$	207.0652	0.0464	192, 175, 157, 147, 119, 91	50	UP	2.1	0.01939	Vinyl caffeate	METLIN ID: 86482
		220.0824	$[M+H]^+$	$C_9H_{17}ONS_2$	220.0824	-0.1640	193	50	UP	1.2	0.00160	1-Isothiocyanato-7-(methylsulfinyl)-heptane	MassBank Record: PR101035
		223.0599	$[M+H]^+$	$C_{10}H_4N_7$	223.0601	-0.8959	208, 167, 163, 135, 107, 79	50	UP	1.9	0.00952	-	
		226.0792	$[M+H]^+$	$C_5H_{15}ON_5S_2$	226.0791	0.3797	208, 193, 176, 148, 120, 119, 92	50	UP	2.7	0.00197	-	
		275.2003	$[M+H]^+$	$C_{18}H_{26}O_2$	275.2006	-0.9535	147, 133, 119, 107, 105, 91, 79, 55	50	DOWN	2.4	0.00587	3,6,9,12,15-octadecapentaenoic acid	METLIN ID: 35023
		277.2159	$[M+H]^+$	$C_{18}H_{28}O_2$	277.2162	-1.0431	149, 135, 121, 107, 95, 93, 81, 79, 67	50	DOWN	3.5	0.00030	Stearidonic Acid	METLIN ID: 34838

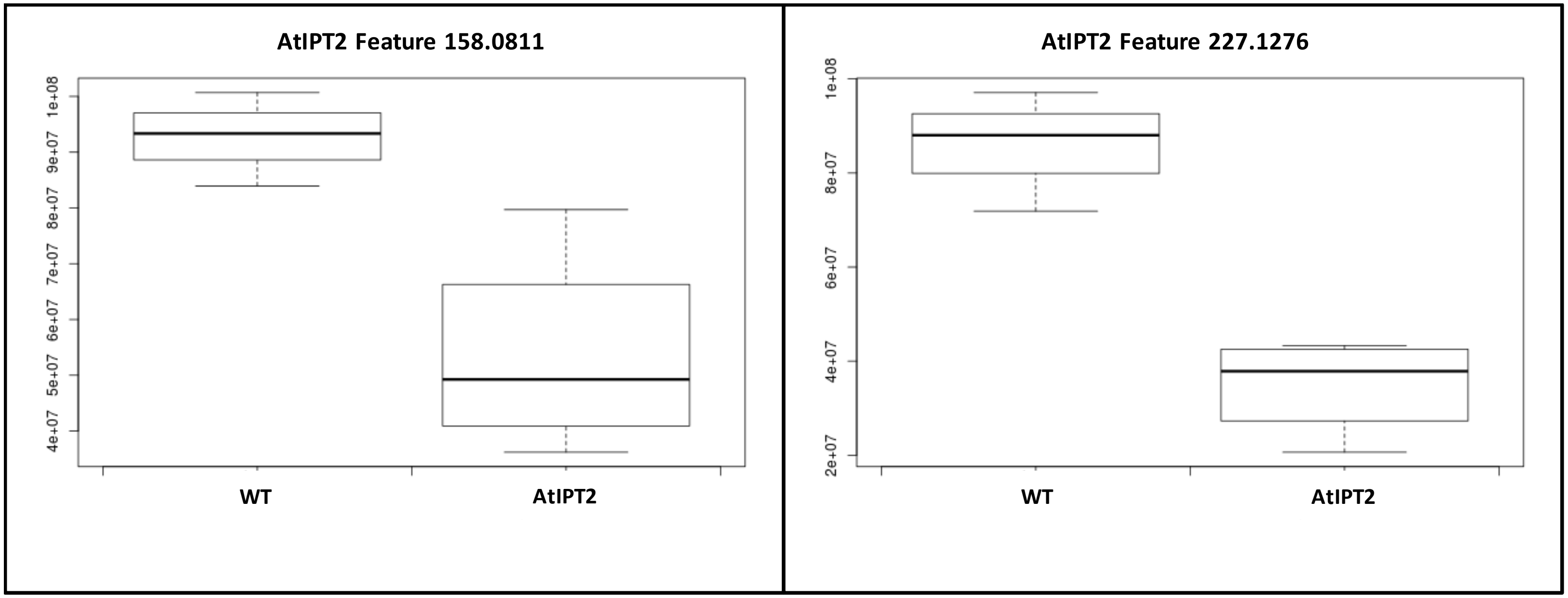

Figure 6: Example Box and whisker plot of metabolite feature *m/z* 158.0811 and 227.1276.

A metabolite feature at *m/z* 207.0652 was found in AtIPT2 during inflorescence and siliques, as well as in seeds of AtIPT9. This feature was upregulated in both mutants' siliques vs WT, 2.7 and 2.1-fold in AtIPT2 and 9 respectively. *m/z* and chemical formula comparison returned a match with vinyl caffeate in METLIN. Vinyl caffeate is a derivative of caffeic acid, which is also a small naturally occurring cinnamic acid. It is involved in plant development of *Arabidopsis*, mainly through the positive regulation of lignin production (Goujon et al., 2003). It has also been shown that the knockout of the gene responsible for the production of caffeic acid affects sinapoyl ester accumulation in seeds, in addition to lignin production (Chapple, 1992). Derivatives of sinapic acid, like sinapoyl esters, are characteristic compounds of the Brassicaceae family (Nićiforović & Abramovič, 2014). This is coincident with ABA levels that were also reduced in the siliques of both mutants. The results closely align with the literature, which shows that an increase in sinapic acid results in a reduction of ABA (Bi, Tang, Han, Guo, & Miao, 2017), as shown in Figure 5 and strongly suggest that *cis*-CK plays a role in maintaining low sinapic acid derivatives and high ABA. This would have the effect of increased seed germination and reduced dormancy depends upon the balance of ABA synthesis and catabolism being shifted towards the former, as well as constant ABA synthesis being required to maintain dormancy (Goggin et al., 2009). Cytokinins play an antagonizing role to ABA in seed germination, promoting seed germination and regulating plant growth (Wang et al., 2011). A reduction in ABA as a result of *cis*-CK suppression would produce seeds that have very little dormancy and quick germination under favorable conditions; whereas higher cis-CK might be normally produced under stress since ABA may also play a role in allowing plants to endure through adverse environmental conditions (Wang et al., 2011).

Feature *m/z* 124.0393 matched on METLIN with nicotinic acid (niacin) by both *m/z*, and predicted chemical formula. This feature was upregulated 2.6-fold in the seeds of AtIPT9. Nicotinic acid is a product of the degradation of nicotinamide adenine dinucleotide (NAD) (Katoh, 2006). Interestingly *m/*z 130.0651 matched with quinoline in both *m/z*, lack of fragmentation, and predicted chemical formula. Homologues for many enzymes involved in alkaloid biosynthesis have been detected in the *Arabidopsis* genome, in spite of the apparent lack of complex alkaloids in this plant; however, a recent discovery that Arabidopsis produces volatile terpenoids, coupled with the multitude of alkaloid biosynthetic gene homologues, lends credibility to the suggestion that undiscovered alkaloids may also be present (Facchini, Bird, & St-Pierre, 2004). Quinoline is a derivative of quinolinic acid, which is a NAD precursor(Katoh, 2006), and it was upregulated in AtIPT9 seeds. NAD overproducing *Arabidopsis* lines have been shown to demonstrate high nicotinic acid, and that the gene expression in those plants is similar to those experiencing biotic stress (Pétriacq et al., 2012). Furthermore, nicotinic acid has been shown to be a growth factor in young pea seedlings, particularly influencing growth of root systems (Bonner, 1937).

A feature at *m/z* 158.0811 returned a match with N-acetyl proline. It was found to be down-regulated in both mutants in first leaves. N-acetyl proline is a derivative of the amino acid proline. It is known to accumulate in plants experiencing drought stress, functioning to increase cell osmolarity (Verslues & Sharma, 2010). Additionally, proline metabolism is associated with plant pathogen interaction as well as programmed cell death (Verslues & Sharma, 2010). Proline may be involved in stress response as it is associated with ornithine synthesis (Kalamaki et al., 2009), which has been attributed to a higher tolerance to salt and drought stress (Winter, Todd, Trovato, Forlani, & Funck, 2015). Considering the reduction in n-acetyl proline in the young mutants, impairment of *cis*-CK may affect the affect the ability for *Arabidopsis* to handle abiotic stressors.

An interesting feature at *m/z* 178.0354 was found downregulated in the inflorescence growth stage of the AtIPT9 mutant, with its product ions found throughout both mutants. The Xcalibur generated chemical formula for the group of precursor ions contained two sulfur atoms, suggesting that the compound may contain a sulfur moiety. When the precursor ion *m/z* 178.0354 was entered into METLIN, a match was found with 4-methylsulfinylbutyl isothiocyanate (sulforaphane) based on *m/z* and the predicted chemical formula. Product ion peaks at *m/z* 114, 72, and 55 were a match with the MS/MS spectra in METLIN, suggesting an identification. MassBank was then searched with a product ion list with corresponding relative intensities to double check the METLIN match. Again, a match with sulforaphane was noted. The feature at *m/z* 114.0372 matches with 4-Isothiocyanato-1-butene on METLIN, along with a match with the predicted chemical formula. This feature shares a similar structure to that of sulforaphane. It was downregulated 1.8-fold, a magnitude similar to that of sulforaphane itself, and was found in the same growth stage. Interestingly the *m/z* 114.0372 feature in seeds of AtIPT2 was upregulated 1.4-fold vs WT. Feature *m/z* 176.0562 matched with 1-Isothiocyanato-5-(methylthio)-pentane on METLIN with both structure and proposed formula. Again, this feature shares a similar structure to sulforaphane, and was upregulated in seeds of the AtIPT9 mutant. Glucosinolates (GL) are precursors to isothiocyanates (ITC) such as sulforaphane and 4-Isothiocyanato-1-butene. ITCs are generated by plants belonging to the Brassicales order when the GLs are degraded (Urbancsok, Bones, & Kissen, 2017). ITCs are located within the vacuole of plant cell, whereas the enzyme myrosinase (KEGG enzyme EC 3.2.1.147) which catalyzes their synthesis is localized to the interior of myrosin grains (Höglund, Lenman, & Rask, 1992), so tissue rupture is a must to bring them into contact.(Gu, Guo, & Gu, 2012). This proposes a mechanism to support the belief that GLs are active against insect herbivores (Hopkins, van Dam, & van Loon, 2009). They have also been associated with defense against microbial pathogens (Bednarek et al., 2009). Additionally, growth in *Arabidopsis* is inhibited by GL derived ITCs, with their side chains influencing the strength of the effect (Urbancsok et al., 2017).

Another metabolite quite similar in structure to that of sulforphane, was found in the seeds of AtIPT2 and AtIPT9. Precursor ion *m/z* 220.0824 and its product ions were entered into MassBank and a match with 1-Isothiocyanato-7-(methylsulfinyl)-heptane was observed, which is another compound in the family of isothiocyanates. Common product ions *m/z* 114 and 55 are in line with the similar structures of these two features. The notable fragment which sets them apart is *m/z* 69. This is a common fragment with a chemical formula of C_5H_9. This sets apart 1-Isothiocyanato-7-(methylsulfinyl)-heptane from sulforaphane, because it contains a longer 7C (vs 4C in sulforaphane) saturated hydrocarbon chain between sulfur moieties. Both features were downregulated vs WT, with sulforaphane reduced 1.8-fold, and 1-Isothiocyanato-7-(methylsulfinyl)-heptane reduced 1.3-fold. In the literature, isothiocyanates have been associated with the Hypersensitive Response (HR) of Arabidopsis, and are thought to induce cell death, and may help with local defense responses (Andersson et al., 2015) as well as response to abiotic stress, since down regulation of sulforaphane, and upregulation of 4-Isothiocyanato-1-butene, and 1-Isothiocyanato-7-(methylsulfinyl)-heptane was found.

CKs in particular have a well-documented role in leaf senescence (Zwack et al., 2013), as well as the ability to induce programmed cell death (Vescovi et al., 2012). A connection between *cis*-CK and isothiocyanates may suggest a link in the process of programmed cell death. Isothiocyanates were detected in reproductive organs of both mutants with levels seemingly associated with the level of *cis*-CK, elevated levels of ITC were detected in AtIPT2 seeds where low levels of *cis*-CK were detected, and reduced ITC levels in AtIPT9 during inflorescence where increased levels of *cis*-CK were detected. It is possible a reduction in *cis*-CK may allow seed senescence to proceed, facilitating the drying out and cell death in preparation for dormancy. The ratio of *cis*-CK to *trans*-CK has been investigated in lupins by Emery et al., 2000. They showed that high ratios of *cis*-CK: *trans*-CK are associated with early reproductive stages which were as high as 17:1 during anthesis, and were observed to drop below 1:1 in tissues once anthesis was complete. A similar switch from cZ to tZ was observed during the progression of barley kernel set and development (Powell et al 2013). This may help explain the findings here where developing siliques in AtIPT2 contained high levels of ITCs. In general tZ-dominant plants (such as *Arabidopsis*) seem to contain cZ in their seeds, perhaps due to their resistance to degradation by CKX genes, as compared to tZ degradation susceptibility, although more wide-spread analysis is necessary (Hluska, 2017). Dormant seeds have also been shown to contain higher *cis*-CK (R.J. Neil Emery et al., 2000; Gajdošová et al., 2011; Quesnelle & Emery, 2007).

Wider impact for cCK is possible since other hormone systems seem to be affected. A feature at *m/z* 160.0756 which is upregulated in siliques of the AtIPT9 mutant points to interaction of cisZ with other hormones. METLIN returns indole-3-acetaldhyde (IAD) as a possible structure based on *m/z* 160.0756, supported by the predicted chemical formula matching with the database result. Further confidence in the match comes from product ions at *m/z* 117 and 145. These are a convincing match with experimental MS/MS spectra in METLIN. Some low intensity product ion peaks also match at *m/z* 145, 130, and 90, with high mass accuracy for each. Identification of *m/z* 160.0756 as IAD may be evidence of impairment an isoform of Aldehyde Oxidase (AO) enzyme (EC 1.2.3.7) which is associated with the production of abscisic acid (ABA) (Rodríguez-Gacio, Matilla-Vázquez, & Matilla, 2009). ABA was reduced in mutant siliques, and this corroborates the 1.8-fold build-up of IAD, a precursor to ABA, in the siliques of the AtIPT9 mutant. While AO has not been investigated in silique tissue, evidence in *Arabidopsis* root tissue has been seen before. A shortened primary root phenotype in AtIPT2 & AtIPT9 mutants was observed in cZ impaired mutants (Köllmer et al., 2014; K. Miyawaki et al., 2006), along with an *Arabidopsis* mutant called superroot1 which demonstrated overexpression of AO, for which the preferred substrate is I3A. AO catalyzes the final step in the biosynthesis of indole-3-acetic acid (IAA), a highly active auxin, whereby AO converts IAD into IAA. (Seo et al., 1998; Won et al., 2011). Additionally, feature *m/z* 205.0972 matched with L-tryptophan in both *m/z* and predicted formula. It was upregulated 1.9-fold in AtIPT9 during inflorescence. It has been shown that L-tryptophan is used by *Arabidopsis* to produce IAA (Won et al., 2011). The buildup of another IAA precursor further supports cis-CKs role in regulating auxin.

CK, ABA, and auxin are closely linked with each other, as well as with the development of plants. Auxin in particular has been linked to seed development, dormancy, and germination in *Arabidopsis*. During seed development auxin acts though coordinated cross-talk with ABA and CKs to facilitate embryo and endosperm communication in seeds. (Locascio, Roig-Villanova, Bernardi, & Varotto, 2014). It has been demonstrated that auxin enhances ABA-mediated seed dormancy by stimulating ABA signaling (X. Liu et al., 2013). The relationship between auxin and CK is often antagonistic in nature. An example of this is during seed development. Levels of auxin are low vs CK, as seed maturation begins the levels reverse with lower levels of CK and greater levels of auxin (Su, Liu, & Zhang, 2011). It appears that auxin, ABA, and CK are closely linked in seed development and maturation, as the results from both CK profiling and metabolite analysis of this thesis suggest that these pathways show cross-talk and have been affected in the mutants, implying there is an important function for cis-CKs.

A pair of features, namely *m/z* 277.2159 and 275.2003 in AtIPT9 siliques, returned matches as highly similar fatty acid derivatives 3,6,9,12,15-octadecapentaenoic acid, and stearidonic acid (6,9,12,15-octadecapentaenoic acid). These features were downregulated 2.4 and 3.5-fold respectively vs WT, indicating a noticeable drop in the concentration of these fatty acids in the seeds of AtIPT9. It has been shown that mutant *Arabidopsis* that produce seeds with reduced seed oil content incorporate alternative carbon sources such as pyruvate and acetate at an increased rate to produce the fatty acids, rather than mainly sucrose and glucose as is the case in WT *Arabidopsis* (Focks & Benning, 1998). It has been demonstrated that exogenous application of ABA causes a dramatic increase in fatty acid accumulation in soybean seed, while exogenous application of tZ causes a moderate increase of fatty acid (Nguyen, 2015). The downregulation of fatty acids coupled with the drop in ABA in the AtIPT9 mutant are well aligned with these observations and thus the idea that cCK promotes fatty acid accumulation in seeds. This is a result that would be of high interest for agronomy and seed quality.

In AtIPT2 first leaves, the featureat *m/z* 227.1278 matched with 12-hydroxyjasmonate with both *m/z* and predicted formula. This feature was downregulated 2.5-fold. Arabidopsis has been demonstrated to contain a specific hydroxy jasmonate sulfotransferase which performs hydroxylation and sulfonation reactions that might be components of a pathway that inactivates excess jasmonic acid in plants (Gidda et al., 2003). Jasmonic acid mediates diverse developmental processes and plant defense responses, so a downregulation of jasmonic acid's active form in a cis-CK impaired mutant suggests that cis-CK may play a role in defense response.

3.5 Summary, Conclusions, and Future Work

The close examination of *cis*-CK impaired AtIPT2 and 9 *Arabidopsis* mutants presented here provides insight into the role *cis*-CKs play in a model plant species. Deviations in trichome development, fresh weight, rosette growth, shoot height, flowering, and suppressed carotenoids all manifested in the mutants as a result of *cis*-CK impairment, indicating the tRNA-degradation CK synthesis pathway has significant impact on plant development. Furthermore, metabolomic analysis showed a number of metabolite features in mutants that differ between the AtIPT2 and AtIPT9 mutants vs WT. Some of the metabolite features that were identified have been associated with CK, auxin, and ABA activity previously, linking the impairment of *cis*-CK to hormone cross-talk and metabolic processes that occur in *Arabidopsis*. So, in addition to the visual phenotypes, cis-CK appears to uphold seed dormancy processes, and affect fatty acid synthesis that have ramifications for seed quality, seed set and germination. The results suggest cis-CKs may be involved during plant reproductive processes, with impacts on both the visible phenotype and metabolite profile hinting at important roles in flowering and silique development. Moreover, key metabolites that are impaired by AtIPT2 and AtIPT9 mutants are related to abiotic and biotic stress suggesting cis-CK represent general stress resistance forms of CK.

Overall, therefore, results suggest we should be paying close attention to cis-CK from the tRNA-degradation pathway as they are potentially of strong interest to the agronomic community on several fronts. As per Gajdošová et al., 2011, Hluska, 2017, and Schäfer et al., 2015, the more one studies cis-CK, the greater the complexity of their roles in plants becomes apparent. The time has come to discard the null hypothesis that cis-CK have negligible effects in plant development. The supporting evidence from both phenotyping and metabolomic analysis support the hypothesis that independently silencing AtIPT2 and 9 genes responsible for *cis*-CK production has an effect on plant development.

Subtle, yet significant, spatial and developmental changes in CK profile were detected by LC-MS in mutants. These changes proved to be important as several of them aligned with phenotype and metabolome impacts in the mutants. That more changes were not found likely reflects that AtIPTs are a multigene family. Thus, it is possible redundancy with other AtIPT genes (either *de novo* or tRNA-IPT) may facilitate the compensation of *cis*-CK suppression, and help mitigate the effects. Limitations on the resolution of the instrument may also factor into the subtleness of the hormone changes, as CKs in general are detected at very low levels. At the phenotype level these subtle changes seem to make a noticeable impact, playing key roles in *Arabidopsis* growth and development. At metabolite level, the metabolites identified here seem to point to *cis*-CK impairment affecting seed viability and dormancy, possible impact on fatty acid synthesis, and biotic and abiotic stress response may be affected.

Repeating these experiments with a double AtIPT2,9 mutant would be beneficial towards the understanding of the role *cis*-CK plays in the development of *Arabidopsis.* This mutant was not available commercially nor through networking (Sakakibara personal communication) at the time of this thesis. The double mutant would provide information about complete t-RNA degradation pathway impairment, possibly elucidating more obvious or impactful phenotypic or metabolism changes. A look at the root tissue at multiple growth stages would also help further the understanding of *cis*-CK involvement in development. Further investigation into the proteomics and genome expression of AtIPT2 and 9 genes would bring with it the finer details of the t-RNA degradation and pathways regulated by AtIPT2 and AtIPT9 in *Arabidopsis*, by providing information about the transcription of AtIPT2 and AtIPT9 genes and protein formation and usage of those proteins affecting the metabolite pool.

Appendix

Table 3: CK and ABA concentration (pmol/gfwt) in WT, AtIPT2 and AtIPT9. The absence of a value indicates CKs that were not detected.

Ecotype	Stage	ABA	DZ	tZ	cisZ	iP	BA	DZR	tZR	cisZR	iPR	DZNT	tZNT	cisZNT	iPNT	MeSZ	MeSiP	MeSZR	MeSiPA	DZOG	DZROG	tZROG	cisZROG	DZ9G	tZOG	cisZOG	tZ9G	cisZ9G	tZ7G
WT	First Leaves	48.0838			0.5274			0.2825	1.1467	0.3920	2.3300		7.5467	4.8181	152.4189	1.8722						0.8096	1.5766		3.3053		3.9734		17.5323
	First Leaves	28.3506			1.7353			0.3911	1.7236	1.0762	3.6415		6.6535	2.6492	100.6302	1.7059						1.2089	1.6020		2.8976		4.2442		15.8831
	First Leaves	35.1310			0.7587			0.1622	1.6922	0.4394	2.9935		9.4604	1.7592	108.0954	1.7897						0.8287	1.1186		6.5306		3.7517		16.4828
	First Leaves	36.1587			1.8269			0.1830	4.5542	0.4000	4.8687		18.2342	2.5906	147.8690	0.8422						1.2463	1.3894		4.9386		6.0616		21.3419
	Inflorescence	33.5198						12.2403	0.2243	0.5077	1.0521					2.9558						2.0765	16.3275		8.2337	1.9598	1.5183		15.8772
	Inflorescence	39.8874						13.4026	0.1674	0.3499	0.8489					3.9429						1.4410	12.3986		8.4781	2.6248	3.1508		21.1751
	Inflorescence	57.1807						13.5182	0.0370	0.4066	0.8200					3.5231						1.4037	12.0777		8.9934	1.8511	2.6399		24.5635
	Inflorescence	39.5243						11.6920	0.2143	0.3361	0.6559					2.7534						0.9018	11.3487		9.2526	2.1771	3.0329		18.7636
	Silique	350.2088		0.6162			1.7193	2.4587	6.8607	3.8405	1.2352		25.3562	11.8597	52.2876	26.6561					9.5370	9.1192			2.6212				
	Silique	292.2099		0.7227			1.6887	2.4840	7.4811	3.3712	1.9261		27.1306	10.5461	61.2570	24.6934					7.9060	8.8537			4.5763				
	Silique	233.4967		0.6510			2.3675	2.5662	6.5221	3.6930	1.8151		24.7033	11.7255	62.5115	27.7541					8.0251	8.2112			3.4630				
	Silique	214.0115		0.5742			1.2414	1.8592	8.0596	2.6279	2.0097		29.8412	9.0305	57.3522	23.5839					8.5675	8.1658			1.4106				
	Seed	1508.6985	24.9772	185.5676	151.5579	19564.3424	2966.7230	10.4719	9.3155	22.6847						25.5881	45.3977	47.8818											
	Seed	1178.7586	10.9854	106.9321	107.5659	8513.9040	1178.6626	9.1675	11.1444	25.1596						11.9048	15.5685	47.7602											
	Seed	1047.4091	22.7932	137.0436	124.9859	12751.9850	4180.9767	9.9301	10.2430	33.7911						17.5899	25.4736	39.4660											
	Seed		1.7576	104.5100	97.5710	15674.4541	675.0102	12.2203	15.7449	57.6947						22.0551	27.7270	46.5989											
IPT2	First Leaves	40.9345							1.7836	0.3536	3.6106		8.6869	0.6430	104.8437	1.7508						0.9012	0.3290		1.8913		4.9912		19.6083
	First Leaves	41.0298							0.6818	0.1003	1.5370		2.7836	0.3780	49.7695	1.9473						0.8347	0.3663		1.9621		2.4172		21.2423
	First Leaves	54.9656							2.4026		2.9299		13.6294	0.4013	114.6739	1.1118						0.8238	0.1671		2.8540		5.8368		15.0595
	First Leaves	58.1813							0.5307	0.1587	1.0066		2.9465	0.3073	33.0762	1.4192						0.6091	0.3358		2.7424		2.6048		13.5880
	Inflorescence	111.5826						14.5905	0.1574		0.6839					3.1244						1.7419	2.9685		3.9705	0.8317	4.2333		35.2054
	Inflorescence	49.7164						9.2384	0.1289	0.6926	0.5718					3.6996						1.8194	17.9194		13.0468	4.7251	2.6727		16.5279
	Inflorescence	25.6947						9.0510	0.2623	0.0682	0.8756					2.6249						2.0356	1.9079		8.0507	0.7977	5.5946		28.7814
	Inflorescence	32.2342						24.0357	0.2701	0.2115	0.6788					3.8430						1.1393	3.3295		6.0103	1.0238	5.6097		24.3579
	Silique	206.3056		0.5876	0.4447		3.4306	2.7805	6.6880	0.4264	1.9246		18.0225	0.6043	53.2675	46.6485					9.9369	6.4710			1.3178				
	Silique	188.6695		0.7518	0.5081		2.4869	2.6957	8.1359	0.8014	2.4285		17.8997	0.7401	69.3741	40.3559					10.7415	7.5447			4.7798				
	Silique	208.9726		0.6492	0.2951		3.4288	2.5906	8.2120	0.6413	2.2088		19.7309	0.8999	47.7949	38.3439					7.6442	9.3191			3.3497				
	Silique	181.1370		0.5129	0.3915		2.4865	2.3138	6.8234	0.5357	1.9646		13.9006	1.2603	62.9382	33.9203					11.4375	8.6651			2.9156				
	Seed	1108.8821	14.2950	96.8467	104.5122	14793.5596	1768.8714	9.3357	22.1708	0.2482						15.6515	21.3029	54.6714											
	Seed	925.4102	5.8093	84.5525	95.4294	12920.7242	913.0300	6.5939	41.4905	5.4202						21.4613	26.5909	107.2671											
	Seed	837.9521	25.8620	421.3924	382.7655	39376.7476	1659.4275	7.5950	31.5200	2.4396						48.3090	82.4217	113.4567											
	Seed		4.8609	107.2908	109.5866	9942.2969	440.9761	7.5453	21.7015	4.9634						14.4812	25.5091	81.7038											
IPT9	First Leaves	42.8178			0.9195				2.3159	0.3951	2.4355		12.2761	1.5239	90.9647	1.4805						0.9893	1.1309		4.0370		2.8788		25.8796
	First Leaves	48.3013			0.3782				1.1316	0.3130	1.3344		8.0210	1.5980	56.8608	1.3450						0.4735	1.2884		6.2842		3.0468		17.3859
	First Leaves	28.6929			0.7279				1.2734	0.4238	1.9615		8.8747	2.1102	60.2515	1.4023						0.8726	1.2025		5.3876		5.7243		20.7983
	First Leaves	63.3124			0.7863				1.3178	0.5688	1.7202		6.8242	1.7061	55.2299	2.2121						0.9012	1.4772		3.8931		5.0478		22.1491
	Inflorescence	41.8022						5.3574	0.4552	0.7082	0.7558					2.8930						1.0765	9.5277		6.3027	0.9146	2.6155		19.2086
	Inflorescence	207.6624						16.9427	0.3095	0.3015	0.6375					3.5781						1.4866	3.6593		5.7716	1.4226	4.1055		28.2980
	Inflorescence	40.2710						6.0335	0.2038	0.6755	0.9077					4.1008						1.5641	12.3140		14.8107	2.2729	4.0442		16.3620
	Inflorescence	52.0180						5.9422	0.1922	0.4690	0.5125					3.6195						1.1738	13.3667		12.4242	2.2564	3.0991		16.3399
	Silique	208.7254		0.5473			2.4066	3.7076	7.9638	4.1801	3.2677		15.1142	12.4590	57.4400	33.4393					12.5804	11.1380			3.7826				
	Silique	229.9367		0.5141			3.7303	4.7471	7.0607	6.1342	3.7122		17.4654	15.2692	58.0766	37.7713					19.3151	8.5818			3.5492				
	Silique	199.8230		0.8134			2.6144	3.6834	10.0447	6.2418	3.9810		14.7458	14.4245	58.0332	29.6811					14.9192	9.5422			6.8603				
	Silique	220.1444		0.5186			2.9650	3.7127	6.2875	4.2903	3.3359		14.7424	11.3685	60.2181	33.7785					13.5924	7.6339			4.0776				
	Seed	811.6232	8.9680	115.0478	102.8609	9642.0560	461.1070	6.9957	20.2120	50.3179						19.7430	22.7491	102.5544											
	Seed	821.6965	8.2144	123.0962	117.7220	11176.5723		9.6310	22.5076	56.8344						19.8121	22.4070	79.4425											
	Seed	1012.1725	1.4691	106.9655	89.4937	8191.0925	1403.5457	10.8046	25.2631	59.1760						28.4764	33.0840	97.0475											
	Seed	1786.8443	3.1120	111.6585	89.8168	8640.6126	27.3533	7.9468	21.3338	44.4893						20.8778	18.8328	81.5901											

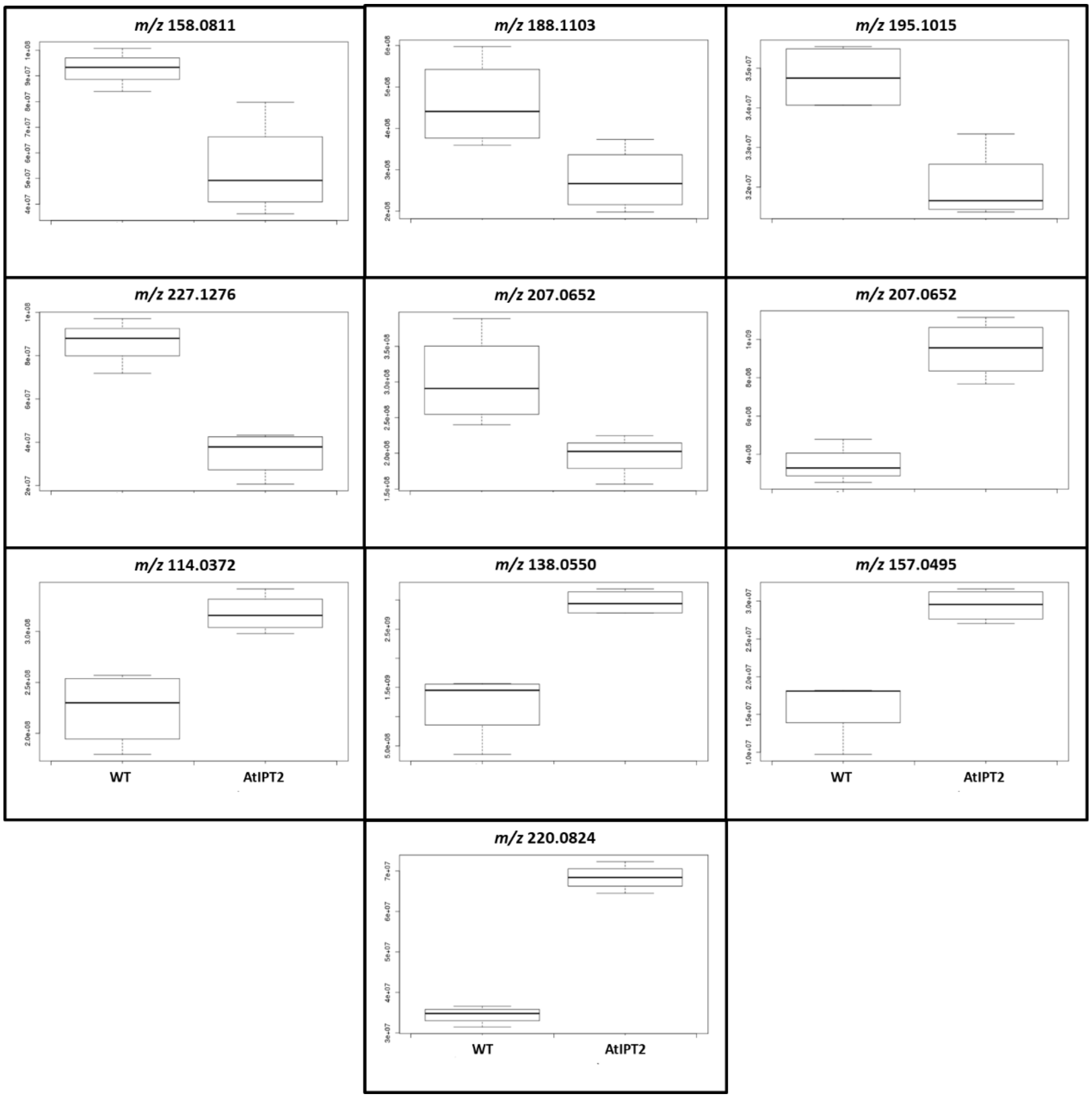

Figure 7: Box and whisker plots of significant AtIPT2 metabolites.

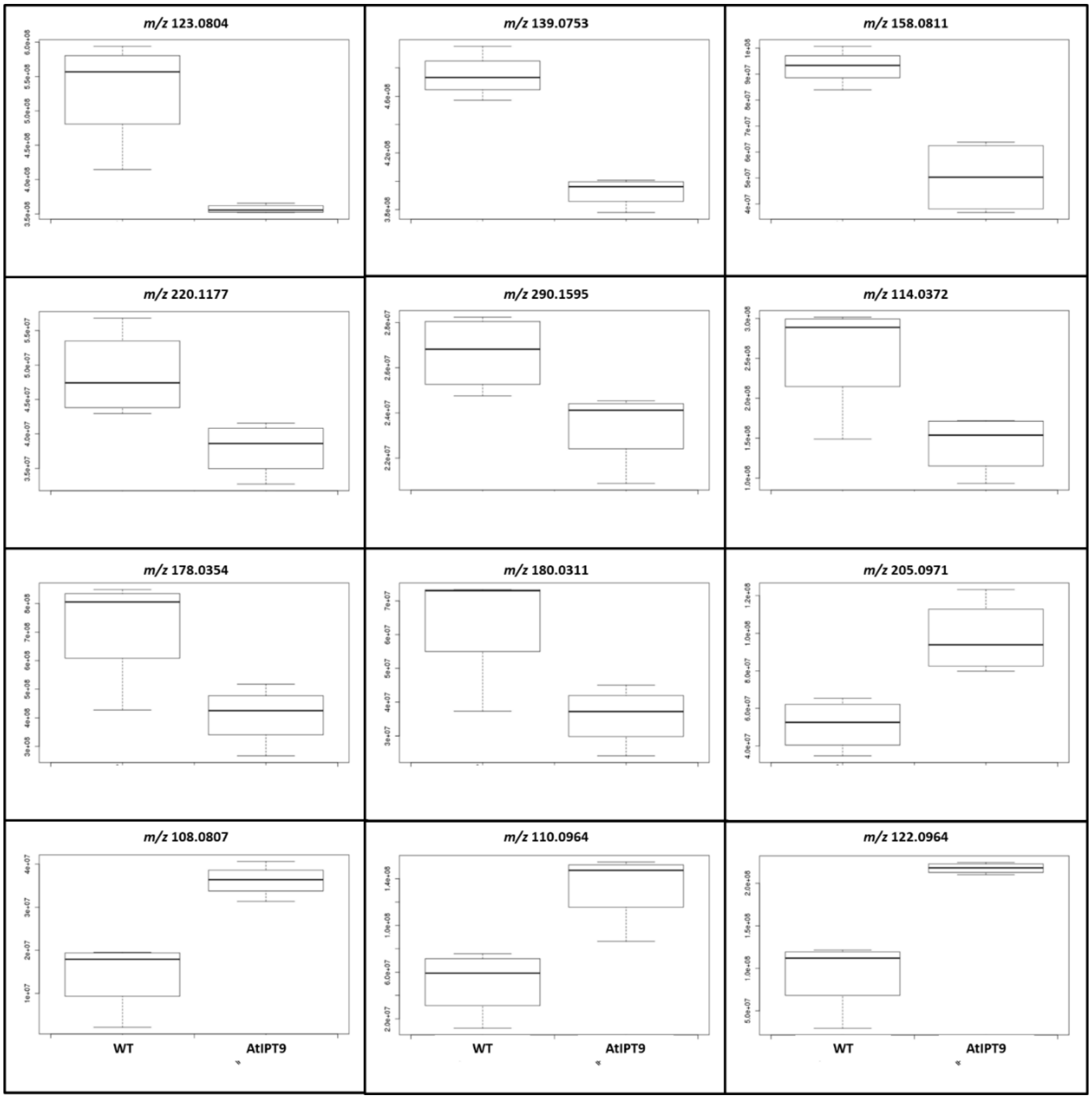

Figure 8: Box and whisker plots of significant AtIPT9 metabolites.

Figure 8: Box and whisker plots of significant AtIPT9 metabolites (continued).

References

Ahn, K. (2017). The worldwide trend of using botanical drugs and strategies for developing global drugs. *BMB Reports*, *50*(3), 111–116. https://doi.org/10.5483/BMBRep.2017.50.3.221

Alonso, J. M., Stepanova, A. N., Leisse, T. J., Kim, C. J., Chen, H., Shinn, P., … Ecker, J. R. (2003). Genome-wide insertional mutagenesis of Arabidopsis thaliana. *Science*, *301*(5633), 653–657. https://doi.org/10.1126/science.1086391

Alvarado, M. C., Zsigmond, L. M., Kovács, I., Cséplö, A., Koncz, C., & Szabados, L. M. (2004). Gene trapping with firefly luciferase in Arabidopsis. Tagging of stress-responsive genes. *Plant Physiology*, *134*(1), 18–27. https://doi.org/10.1104/pp.103.027151

An, L., Zhou, Z., Yan, A., & Gan, Y. (2011). Progress on trichome development regulated by phytohormone signaling. *Plant Signaling and Behavior*, *6*(12), 1959–1962. https://doi.org/10.4161/psb.6.12.18120

Andersson, M. X., Nilsson, A. K., Johansson, O. N., Boztaş, G., Adolfsson, L. E., Pinosa, F., … Ellerström, M. (2015). Involvement of the Electrophilic Isothiocyanate Sulforaphane in Arabidopsis Local Defense Responses. *Plant Physiology*, *167*(1), 251–261. https://doi.org/10.1104/pp.114.251892

Bednarek, P., Piślewska-Bednarek, M., Svatoš, A., Schneider, B., Doubský, J., Mansurova, M., … Schulze-Lefert, P. (2009). A glucosinolate metabolism pathway in living plant cells mediates broad-spectrum antifungal defense. *Science*, *323*(5910), 101–106. https://doi.org/10.1126/science.1163732

Bernier, G. (1993). Physiological Signals That Induce Flowering. *The Plant Cell Online*, *5*(10), 1147–1155. https://doi.org/10.1105/tpc.5.10.1147

Bi, B., Tang, J., Han, S., Guo, J., & Miao, Y. (2017). Sinapic acid or its derivatives interfere with abscisic acid homeostasis during Arabidopsis thaliana seed germination. *BMC Plant Biology*, *17*(1), 1–12. https://doi.org/10.1186/s12870-017-1048-9

Bonner, J. (1937). Nictotinic acid and the growth of isolated pea embyos. *Plant Physiology*, (465), 865–868.

Bouché, N., & Bouchez, D. (2001). Arabidopsis gene knockout: Phenotypes wanted. *Current Opinion in Plant Biology*, *4*(2), 111–117. https://doi.org/10.1016/S1369-5266(00)00145-X

Boyes, D. C. (2001). Growth Stage-Based Phenotypic Analysis of Arabidopsis: A Model for High Throughput Functional Genomics in Plants. *The Plant Cell Online*, *13*(7), 1499–1510. https://doi.org/10.1105/tpc.13.7.1499

Bundy, J. G., Davey, M. P., & Viant, M. R. (2009). Environmental metabolomics: A critical review and future perspectives. *Metabolomics*, *5*(1), 3–21. https://doi.org/10.1007/s11306-008-0152-0

Chapple, C. (1992). An Arabidopsis Mutant Defective in the General Phenylpropanoid Pathway. *The Plant Cell Online*, *4*(11), 1413–1424. https://doi.org/10.1105/tpc.4.11.1413

Chen, C., Li, C., Wang, Y., Renaud, J., Tian, G., Kambhampati, S., … Cui, Y. (2017). Cytosolic acetyl-CoA promotes histone acetylation predominantly at H3K27 in

Arabidopsis. *Nature Plants*, *3*(10), 814–824. https://doi.org/10.1038/s41477-017-0023-7
D'Aloia, M., Bonhomme, D., Bouché, F., Tamseddak, K., Ormenese, S., Torti, S., … Périlleux, C. (2011). Cytokinin promotes flowering of Arabidopsis via transcriptional activation of the FT paralogue TSF. *Plant Journal*, *65*(6), 972–979. https://doi.org/10.1111/j.1365-313X.2011.04482.x
De Vos, R. C. H., Moco, S., Lommen, A., Keurentjes, J. J. B., Bino, R. J., & Hall, R. D. (2007). Untargeted large-scale plant metabolomics using liquid chromatography coupled to mass spectrometry. *Nature Protocols*, *2*(4), 778–791. https://doi.org/10.1038/nprot.2007.95
Dello Ioio, R., Galinha, C., Fletcher, A. G., Grigg, S. P., Molnar, A., Willemsen, V., … Tsiantis, M. (2012). A PHABULOSA/cytokinin feedback loop controls root growth in arabidopsis. *Current Biology*, *22*(18), 1699–1704. https://doi.org/10.1016/j.cub.2012.07.005
Emery, R. J. N., Leport, L., Barton, J. E., Turner, N. C., & Atkins, C. A. (1998). cis-Isomers of Cytokinins Predominate in Chickpea Seeds throughout Their Development1. *Plant Physiology*, *117*(4), 1515–1523. https://doi.org/10.1104/pp.117.4.1515
Emery, R. J. N., Ma, Q., & Atkins, C. A. (2000). The Forms and Sources of Cytokinins in Developing White Lupine Seeds and Fruits. *Plant Physiology*, *123*(4), 1593–1604. https://doi.org/10.1104/pp.123.4.1593
Facchini, P. J., Bird, D. A., & St-Pierre, B. (2004). Can Arabidopsis make complex alkaloids? *Trends in Plant Science*, *9*(3), 116–122. https://doi.org/10.1016/j.tplants.2004.01.004
Farrow, S. C., & Emery, R. J. N. (2012). Concurrent profiling of indole-3-acetic acid , abscisic acid , and cytokinins and structurally related purines by high-performance-liquid- chromatography tandem electrospray mass spectrometry Concurrent profiling of indole-3-acetic acid , abscisic acid , . *Plant Methods*, *8*(1), 1. https://doi.org/10.1186/1746-4811-8-42
Focks, N., & Benning, C. (1998). *wrinkled1* : A Novel, Low-Seed-Oil Mutant of Arabidopsis with a Deficiency in the Seed-Specific Regulation of Carbohydrate Metabolism. *Plant Physiology*, *118*(1), 91–101. https://doi.org/10.1104/pp.118.1.91
Frébort, I., Kowalska, M., Hluska, T., Frébortová, J., & Galuszka, P. (2011). Evolution of cytokinin biosynthesis and degradation. *Journal of Experimental Botany*, *62*(8), 2431–2452. https://doi.org/10.1093/jxb/err004
Fukushima, A., Kusano, M., Mejia, R. F., Iwasa, M., Kobayashi, M., Hayashi, N., … Saito, K. (2014). Metabolomic Characterization of Knockout Mutants in Arabidopsis: Development of a Metabolite Profiling Database for Knockout Mutants in Arabidopsis. *Plant Physiology*, *165*(3), 948–961. https://doi.org/10.1104/pp.114.240986
Gajdošová, S., Spíchal, L., Kamínek, M., Hoyerová, K., Novák, O., Dobrev, P. I., … Motyka, V. (2011). Distribution, biological activities, metabolism, and the conceivable function of cis-zeatin-type cytokinins in plants. *Journal of Experimental Botany*, *62*(8), 2827–2840. https://doi.org/10.1093/jxb/erq457
Gazzarrini, S., & Mccourt, P. (2003). Cross-talk in plant hormone signalling: What

arabidopsis mutants are telling us. *Annals of Botany*, *91*(6), 605–612. https://doi.org/10.1093/aob/mcg064

Gidda, S. K., Miersch, O., Levitin, A., Schmidt, J., Wasternack, C., & Varin, L. (2003). Biochemical and molecular characterization of a hydroxyjasmonate sulfotransferase from Arabidopsis thaliana. *Journal of Biological Chemistry*, *278*(20), 17895–17900. https://doi.org/10.1074/jbc.M211943200

Goggin, D. E., Steadman, K. J., Emery, R. J. N., Farrow, S. C., Benech-Arnold, R. L., & Powles, S. B. (2009). ABA inhibits germination but not dormancy release in mature imbibed seeds of Lolium rigidum Gaud. *Journal of Experimental Botany*, *60*(12), 3387–3396. https://doi.org/10.1093/jxb/erp175

Golovko, A., Hjälm, G., Sitbon, F., & Nicander, B. (2000). Cloning of a human tRNA isopentenyl transferase. *Gene*, *258*(1–2), 85–93. https://doi.org/10.1016/S0378-1119(00)00421-2

Goujon, T., Sibout, R., Pollet, B., Maba, B., Nussaume, L., Bechtold, N., … Jouanin, L. (2003). A new Arabidopsis thaliana mutant deficient in the expression of O-methyltransferase impacts lignins and sinapoyl esters. *Plant Molecular Biology*, *51*(6), 973–989. https://doi.org/10.1023/A:1023022825098

Grotz, N., Fox, T., Connolly, E., Park, W., Guerinot, M. L., & Eide, D. (1998). Identification of a family of zinc transporter genes from Arabidopsis that respond to zinc deficiency. *Proceedings of the National Academy of Sciences*, *95*(12), 7220–7224. https://doi.org/10.1073/pnas.95.12.7220

Gu, Z. xin, Guo, Q. hui, & Gu, Y. juan. (2012). Factors Influencing Glucoraphanin and Sulforaphane Formation in Brassica Plants: A Review. *Journal of Integrative Agriculture*, *11*(11), 1804–1816. https://doi.org/10.1016/S2095-3119(12)60185-3

Hashizume, T., Sugiyama, T., Imura, M., Cory, H. T., Scott, M. F., & McCloskey, J. A. (1979). Determination of cytokinins by mass spectrometry based on stable isotope dilution. *Analytical Biochemistry*, *92*(1), 111–122. https://doi.org/10.1016/0003-2697(79)90631-6

Hirose, N., Takei, K., Kuroha, T., Kamada-Nobusada, T., Hayashi, H., & Sakakibara, H. (2008). Regulation of cytokinin biosynthesis, compartmentalization and translocation. *Journal of Experimental Botany*, *59*(1), 75–83. https://doi.org/10.1093/jxb/erm157

Hiscox, J. D., & Israelstam, G. F. (1979). A method for the extraction of chlorophyll from leaf tissue without maceration. *Canadian Journal of Botany*, *57*(12), 1332–1334. https://doi.org/10.1139/b79-163

Hluska, T. (2017). Metabolism of Zeatin-Type Cytokinins in Monocotyledonous Plants.

Höglund, A. S., Lenman, M., & Rask, L. (1992). Myrosinase is localized to the interior of myrosin grains and is not associated to the surrounding tonoplast membrane. *Plant Science*, *85*(2), 165–170. https://doi.org/10.1016/0168-9452(92)90112-Y

Hopkins, R. J., van Dam, N. M., & van Loon, J. J. A. (2009). Role of Glucosinolates in Insect-Plant Relationships and Multitrophic Interactions. *Annual Review of Entomology*, *54*(1), 57–83. https://doi.org/10.1146/annurev.ento.54.110807.090623

Hwang, I., & Sheen, J. (2001). Two-component circuitry in *Arabidopsis* cytokinin signal

transduction. *Nature*, *413*(6854), 383–389. https://doi.org/10.1038/35096500
Kalamaki, M. S., Alexandrou, D., Lazari, D., Merkouropoulos, G., Fotopoulos, V., Pateraki, I., … Kanellis, A. K. (2009). Over-expression of a tomato N-acetyl-L-glutamate synthase gene (SlNAGS1) in Arabidopsis thaliana results in high ornithine levels and increased tolerance in salt and drought stresses. *Journal of Experimental Botany*, *60*(6), 1859–1871. https://doi.org/10.1093/jxb/erp072
Kamada-Nobusada, T., & Sakakibara, H. (2009). Molecular basis for cytokinin biosynthesis. *Phytochemistry*, *70*(4), 444–449. https://doi.org/10.1016/j.phytochem.2009.02.007
Kambhampati, S., Kurepin, L. V., Kisiala, A. B., Bruce, K. E., Cober, E. R., Morrison, M. J., & Emery, R. J. N. (2017). Yield associated traits correlate with cytokinin profiles in developing pods and seeds of field-grown soybean cultivars. *Field Crops Research*, *214*(September), 175–184. https://doi.org/10.1016/j.fcr.2017.09.009
Kasahara, H., Takei, K., Ueda, N., Hishiyama, S., Yamaya, T., Kamiya, Y., … Sakakibara, H. (2004). Distinct Isoprenoid Origins of cis- and trans-Zeatin Biosyntheses in Arabidopsis. *Journal of Biological Chemistry*, *279*(14), 14049–14054. https://doi.org/10.1074/jbc.M314195200
Katoh, A. (2006). Early Steps in the Biosynthesis of NAD in Arabidopsis Start with Aspartate and Occur in the Plastid. *Plant Physiology*, *141*(3), 851–857. https://doi.org/10.1104/pp.106.081091
Kerem Bingol, Lei Bruschweiler, Cao Yu, Arpad Somogyi, Fengli Zhang, R. B. (2016). Metabolomics Beyond Spectroscopic Databases: A Combined MS/NMR Strategy for the Rapid Identification of New Metabolites in Complex Mixtures, *48*(0), 923–930. https://doi.org/10.1016/j.clinbiochem.2015.06.023.Gut-Liver
Khan, M., Rozhon, W., & Poppenberger, B. (2013). The role of hormones in the aging of plants - A mini-review. *Gerontology*, *60*(1), 49–55. https://doi.org/10.1159/000354334
Köllmer, I., Novák, O., Strnad, M., Schmülling, T., & Werner, T. (2014). Overexpression of the cytosolic cytokinin oxidase/dehydrogenase (CKX7) from Arabidopsis causes specific changes in root growth and xylem differentiation. *Plant Journal*, *78*(3), 359–371. https://doi.org/10.1111/tpj.12477
Leng, G., & Huang, M. (2017). Crop yield response to climate change varies with crop spatial distribution pattern. *Scientific Reports*, *7*(1), 1–10. https://doi.org/10.1038/s41598-017-01599-2
Lindner, A. C., Lang, D., Seifert, M., Podlešáková, K., Novák, O., Strnad, M., … Von Schwartzenberg, K. (2014). Isopentenyltransferase-1 (IPT1) knockout in Physcomitrella together with phylogenetic analyses of IPTs provide insights into evolution of plant cytokinin biosynthesis. *Journal of Experimental Botany*, *65*(9), 2533–2543. https://doi.org/10.1093/jxb/eru142
Liu, Q., Shi, Y., Guo, T., Wang, Y., Cong, W., & Zhu, J. (2012). Metabolite discovery of helicidum in rat urine with XCMS based on the data of ultra performance liquid chromatography coupled to time-of-flight mass spectrometry. *Journal of Chromatography B: Analytical Technologies in the Biomedical and Life Sciences*, *907*, 146–153. https://doi.org/10.1016/j.jchromb.2012.09.029

Liu, X., Zhang, H., Zhao, Y., Feng, Z., Li, Q., Yang, H.-Q., … He, Z.-H. (2013). Auxin controls seed dormancy through stimulation of abscisic acid signaling by inducing ARF-mediated ABI3 activation in Arabidopsis. *Proceedings of the National Academy of Sciences*, *110*(38), 15485–15490. https://doi.org/10.1073/pnas.1304651110

Locascio, A., Roig-Villanova, I., Bernardi, J., & Varotto, S. (2014). Current perspectives on the hormonal control of seed development in Arabidopsis and maize: a focus on auxin. *Frontiers in Plant Science*, *5*(August), 1–22. https://doi.org/10.3389/fpls.2014.00412

Maruyama, K., Sakuma, Y., Kasuga, M., Ito, Y., Seki, M., Goda, H., … Yamaguchi-Shinozaki, K. (2004). Identification of cold-inducible downstream genes of the Arabidopsis DREB1A/CBF3 transcriptional factor using two microarray systems. *Plant Journal*, *38*(6), 982–993. https://doi.org/10.1111/j.1365-313X.2004.02100.x

Matías-hernández, L., Aguilar-jaramillo, A. E., Cigliano, R. A., Sanseverino, W., & Pelaz, S. (2016). Flowering and trichome development share hormonal and transcription factor regulation, *67*(5), 1209–1219. https://doi.org/10.1093/jxb/erv534

Mauk, C. S., & Langille, A. R. (1978). Physiology of Tuberization in Solanum tuberosum L: cis-Zeatin Riboside in the Potato Plant: Its Identification and Changes in Endogenous Levels as Influenced by Temperature and Photoperiod. *Plant Physiology*, *62*(3), 438–442. https://doi.org/10.1104/pp.62.3.438

Miyawaki, K., Matsumoto-Kitano, M., & Kakimoto, T. (2004). Expression of cytokinin biosynthetic isopentenyltransferase genes in Arabidopsis: Tissue specificity and regulation by auxin, cytokinin, and nitrate. *Plant Journal*, *37*(1), 128–138. https://doi.org/10.1046/j.1365-313X.2003.01945.x

Miyawaki, K., Tarkowski, P., Matsumoto-Kitano, M., Kato, T., Sato, S., Tarkowska, D., … Kakimoto, T. (2006). Roles of Arabidopsis ATP/ADP isopentenyltransferases and tRNA isopentenyltransferases in cytokinin biosynthesis. *Proceedings of the National Academy of Sciences*, *103*(44), 16598–16603. https://doi.org/10.1073/pnas.0603522103

Mok, D. W. S., & Mok, M. C. (2001). Cytokinin Metabolism and Action, 89–118.

Morrison, E. N., Emery, R. J. N., & Saville, B. J. (2017). Fungal derived cytokinins are necessary for normal Ustilago maydis infection of maize. *Plant Pathology*, *66*(5), 726–742. https://doi.org/10.1111/ppa.12629

Navarro-Reig, M., Jaumot, J., García-Reiriz, A., & Tauler, R. (2015). Evaluation of changes induced in rice metabolome by Cd and Cu exposure using LC-MS with XCMS and MCR-ALS data analysis strategies. *Analytical and Bioanalytical Chemistry*, *407*(29), 8835–8847. https://doi.org/10.1007/s00216-015-9042-2

Nguyen, T. Q. (2015). THE INVOLVEMENT OF ENDOGENOUS PLANT HORMONES IN THE REGULATORY NETWORK OF FATTY ACID BIOSYNTHESIS IN SOYBEAN SEED.

Nićiforović, N., & Abramovič, H. (2014). Sinapic acid and its derivatives: Natural sources and bioactivity. *Comprehensive Reviews in Food Science and Food Safety*, *13*(1), 34–51. https://doi.org/10.1111/1541-4337.12041

Nishiyama, R., Watanabe, Y., Fujita, Y., Le, D. T., Kojima, M., Werner, T., … Tran, L.-S. P. (2011). Analysis of Cytokinin Mutants and Regulation of Cytokinin Metabolic Genes Reveals Important Regulatory Roles of Cytokinins in Drought, Salt and Abscisic Acid

Responses, and Abscisic Acid Biosynthesis. *The Plant Cell*, *23*(6), 2169–2183. https://doi.org/10.1105/tpc.111.087395

Osugi, A., & Sakakibara, H. (2015). Q&A: How do plants respond to cytokinins and what is their importance? *BMC Biology*, *13*(1), 102. https://doi.org/10.1186/s12915-015-0214-5

Persson, B. C., Esberg, B., Ólafsson, Ó., & Björk, G. R. (1994). Synthesis and function of isopentenyl adenosine derivatives in tRNA. *Biochimie*, *76*(12), 1152–1160. https://doi.org/10.1016/0300-9084(94)90044-2

Pétriacq, P., De Bont, L., Hager, J., Didierlaurent, L., Mauve, C., Guérard, F., … Gakière, B. (2012). Inducible NAD overproduction in Arabidopsis alters metabolic pools and gene expression correlated with increased salicylate content and resistance to Pst-AvrRpm1. *Plant Journal*, *70*(4), 650–665. https://doi.org/10.1111/j.1365-313X.2012.04920.x

Prerostova, S., Dobrev, P. I., Gaudinova, A., Knirsch, V., Körber, N., Pieruschka, R., … Vankova, R. (2018). Cytokinins: Their Impact on Molecular and Growth Responses to Drought Stress and Recovery in Arabidopsis. *Frontiers in Plant Science*, *9*(May), 655. https://doi.org/10.3389/fpls.2018.00655

Queiroz, O., & Morel, C. (1974). Photoperiodism and enzyme activity. *Plant Physiol.*, *53*, 596–602.

Quesnelle, P. E., & Emery, R. J. N. (2007). *cis* -Cytokinins that predominate in *Pisum sativum* during early embryogenesis will accelerate embryo growth in vitro. *Canadian Journal of Botany*, *85*(1), 91–103. https://doi.org/10.1139/b06-149

R. Verpoorte, Y. H. C. and H. K. K. (2007). Metabolomics: what's new? *Flavour and Fragrance Journal*, *22*(November), 206–213. https://doi.org/10.1002/ffj

Renaud, J. B., Sabourin, L., Topp, E., & Sumarah, M. W. (2017). Spectral Counting Approach to Measure Selectivity of High-Resolution LC-MS Methods for Environmental Analysis. *Analytical Chemistry*, *89*(5), 2747–2754. https://doi.org/10.1021/acs.analchem.6b03475

Rodríguez-Gacio, M. D. C., Matilla-Vázquez, M. a, & Matilla, A. J. (2009). Seed dormancy and ABA signaling: the breakthrough goes on. *Plant Signaling & Behavior*, *4*(11), 1035–1049. https://doi.org/10.4161/psb.4.11.9902

Ruiz-Sola, M. Á., & Rodríguez-Concepción, M. (2012). Carotenoid Biosynthesis in Arabidopsis: A Colorful Pathway. *The Arabidopsis Book*, *10*, e0158. https://doi.org/10.1199/tab.0158

Sakakibara, H. (2006). CYTOKININS: Activity, Biosynthesis, and Translocation. *Annual Review of Plant Biology*, *57*(1), 431–449. https://doi.org/10.1146/annurev.arplant.57.032905.105231

Sakakibara, H., Kasahara, H., Ueda, N., Kojima, M., Takei, K., Hishiyama, S., … Yamaguchi, S. (2005). Agrobacterium tumefaciens increases cytokinin production in plastids by modifying the biosynthetic pathway in the host plant. *Proceedings of the National Academy of Sciences of the United States of America*, *102*(28), 9972–9977. https://doi.org/10.1073/pnas.0500793102

Scalbert, A., Brennan, L., Fiehn, O., Hankemeier, T., Kristal, B. S., van Ommen, B., … Wopereis, S. (2009). Mass-spectrometry-based metabolomics: Limitations and recommendations for future progress with particular focus on nutrition research. *Metabolomics*, *5*(4), 435–458. https://doi.org/10.1007/s11306-009-0168-0

Scarbrough, E., Armstrong, D. J., Skoog, F., Frihart, C. R., & Leonard, N. J. (1973). Isolation of cis-Zeatin from Corynebacterium fascians Cultures. *Proceedings of the National Academy of Sciences of the United States of America*, *70*(12 Pt 1-2), 3825–3829. https://doi.org/10.1073/pnas.70.12.3825

Schäfer, M., Brütting, C., Meza-Canales, I. D., Großkinsky, D. K., Vankova, R., Baldwin, I. T., & Meldau, S. (2015). The role of cis -zeatin-type cytokinins in plant growth regulation and mediating responses to environmental interactions. *Journal of Experimental Botany*, *66*(16), 4873–4884. https://doi.org/10.1093/jxb/erv214

Schmitz, R. Y., Skoog, F., Playtis, A. J., & Leonard, N. J. (1972). Cytokinins: Synthesis and Biological Activity of Geometric and Position Isomers of Zeatin. *Plant Physiology*, *50*(6), 702–705. https://doi.org/10.1104/pp.50.6.702

Seegobin, M., Kisiala, A., Noble, A., Kaplan, D., Brunetti, C., & Emery, R. J. N. (2018). *Canis familiaris* tissues are characterized by different profiles of cytokinins typical of the tRNA degradation pathway. *The FASEB Journal*, (15), fj.201800347. https://doi.org/10.1096/fj.201800347

Seo, M., Akaba, S., Oritani, T., Delarue, M., Bellini, C., Caboche, M., & Koshiba, T. (1998). Higher Activity of an Aldehyde Oxidase in the Auxin-Overproducing *superroot1* Mutant of *Arabidopsis thaliana*. *Plant Physiology*, *116*(2), 687–693. https://doi.org/10.1104/pp.116.2.687

Skalický, V., Kubeš, M., & Napier, R. (2018). Auxins and Cytokinins — The Role of Subcellular Organization on Homeostasis. *International Journal of Molecular Sciences*. https://doi.org/10.3390/ijms19103115

Spíchal, L. (2012). Cytokinins - Recent news and views of evolutionally old molecules. *Functional Plant Biology*, *39*(4), 267–284. https://doi.org/10.1071/FP11276

Spíchal, L., Rakova, N. Y., Riefler, M., Mizuno, T., Romanov, G. A., Strnad, M., & Schmülling, T. (2004). Two cytokinin receptors of Arabidopsis thaliana, CRE1/AHK4 and AHK3, differ in their ligand specificity in a bacterial assay. *Plant and Cell Physiology*, *45*(9), 1299–1305. https://doi.org/10.1093/pcp/pch132

Stirk, W. A., & van Staden, J. (2010). Flow of cytokinins through the environment. *Plant Growth Regulation*, *62*(2), 101–116. https://doi.org/10.1007/s10725-010-9481-x

Strzelczyk , E., Pokojska, A., Kampert, M., Michalski, L., Kowalski, S. (1989). Production of plant growth regulators by non-mycorrhizal fungi associated with the roots of forest trees. *Developments in Soil Science*, *18*, 213–222.

Su, Y. H., Liu, Y. B., & Zhang, X. S. (2011). Auxin-cytokinin interaction regulates meristem development. *Molecular Plant*, *4*(4), 616–625. https://doi.org/10.1093/mp/ssr007

Sun, X., Zhang, J., Zhang, H., Ni, Y., Zhang, Q., Chen, J., & Guan, Y. (2010). The responses of Arabidopsis thaliana to cadmium exposure explored via metabolite profiling. *Chemosphere*, *78*(7), 840–845. https://doi.org/10.1016/j.chemosphere.2009.11.045

Suttle, J. C., & Banowetz, G. M. (2000). Changes in cis -zeatin and cis -zeatin riboside levels and biological activity during potato tuber dormancy, 68–74.

Takagi, M., Yokota, T., Murofushi, N., Ota, Y., & Takahashi, N. (1985). Fluctuation of endogenous cytokinin contents in rice during its life cycle—quantification of cytokinins by selected ion monitoring using deuterium-labelled internal standards. *Agricultural and Biological Chemistry*, *49*(11), 3271–3277. https://doi.org/10.1080/00021369.1985.10867233

Takei, K., Sakakibara, H., & Sugiyama, T. (2001). Identification of Genes Encoding Adenylate Isopentenyltransferase, a Cytokinin Biosynthesis Enzyme, in Arabidopsis thaliana. *Journal of Biological Chemistry*, *276*(28), 26405–26410. https://doi.org/10.1074/jbc.M102130200

The Arabidopsis Genome Initiative. (2000). Analysis of the genome sequence of the flowering plant Arabidopsis thaliana. *Nature*, *408*(6814), 796–815. https://doi.org/10.1038/35048692

Tomas Werner, Vaclav Motyka, Miroslav Strnad, and T. S. (2001). Regulation of plant growth by cytokinin, *98*(18), 10487–10492.

Tsutomu Inoue, Masayuki Higuchi, Yukari Hashimoto, Motoaki Seki, Masatomo Kobayashi, Tomohiko Kato, Satoshi Tabata, Kazuo Shinozaki, T. K. (2001). Identification of CRE1 as a cytokinin receptor from Arabidopsis, *248*(February), 48–51.

Urbancsok, J., Bones, A. M., & Kissen, R. (2017). Glucosinolate-Derived Isothiocyanates Inhibit Arabidopsis Growth and the Potency Depends on Their Side Chain Structure. https://doi.org/10.3390/ijms18112372

Veach, Y. K., Martin, R. C., Mok, D. W. S., Malbeck, J., Vankova, R., & Mok, M. C. (2003). O-glucosylation of cis-zeatin in maize. Characterization of genes, enzymes, and endogenous cytokinins. *Plant Physiology*, *131*(3), 1374–1380. https://doi.org/10.1104/pp.017210

Verslues, P. E., & Sharma, S. (2010). Proline Metabolism and Its Implications for Plant-Environment Interaction. *The Arabidopsis Book*, *8*, e0140. https://doi.org/10.1199/tab.0140

Vescovi, M., Riefler, M., Gessuti, M., Novák, O., Schmülling, T., & Lo Schiavo, F. (2012). Programmed cell death induced by high levels of cytokinin in Arabidopsis cultured cells is mediated by the cytokinin receptor CRE1/AHK4. *Journal of Experimental Botany*, *63*(7), 2825–2832. https://doi.org/10.1093/jxb/ers008

Vyroubalova, S., Vaclavikova, K., Tureckova, V., Novak, O., Smehilova, M., Hluska, T., … Galuszka, P. (2009). Characterization of New Maize Genes Putatively Involved in Cytokinin Metabolism and Their Expression during Osmotic Stress in Relation to Cytokinin Levels. *Plant Physiology*, *151*(1), 433–447. https://doi.org/10.1104/pp.109.142489

Wang, Y., Li, L., Ye, T., Zhao, S., Liu, Z., Feng, Y., & Wu, Y. (2011). Cytokinin antagonizes ABA suppression to seed germination of Arabidopsis by downregulating ABI5 expression, 249–261. https://doi.org/10.1111/j.1365-313X.2011.04683.x

Weckwerth, W., & Fiehn, O. (2002). Can we discover novel pathways using metabolomic analysis? *Current Opinion in Biotechnology*, *13*(2), 156–160. https://doi.org/10.1016/S0958-1669(02)00299-9

Wen, H., Cho, H. R., Yun, T., Kim, H., Park, C. K., Lee, S. H., … Park, S. (2015). Metabolomic comparison between cells over-expressing isocitrate dehydrogenase

1 and 2 mutants and the effects of an inhibitor on the metabolism. *Journal of Neurochemistry*, *132*(2), 183–193. https://doi.org/10.1111/jnc.12950

Werner, T., Motyka, V., Laucou, V., Smets, R., Onckelen, H. Van, & Schmuelling, T. (2003). Cytokinin-Deficient Transgenic Arabidopsis Plants Show Functions of Cytokinins in the Regulation of Shoot and Root Meristem Activity. *The Plant Cell*, *15*(November), 2532–2550. https://doi.org/10.1105/tpc.014928.)

Winter, G., Todd, C. D., Trovato, M., Forlani, G., & Funck, D. (2015). Physiological implications of arginine metabolism in plants. *Frontiers in Plant Science*, *6*(July), 1–14. https://doi.org/10.3389/fpls.2015.00534

Won, C., Shen, X., Mashiguchi, K., Zheng, Z., Dai, X., Cheng, Y., … Zhao, Y. (2011). Conversion of tryptophan to indole-3-acetic acid by TRYPTOPHAN AMINOTRANSFERASES OF ARABIDOPSIS and YUCCAs in Arabidopsis. *Proceedings of the National Academy of Sciences*, *108*(45), 18518–18523. https://doi.org/10.1073/pnas.1108436108

Wu, H., Southam, A. D., Hines, A., & Viant, M. R. (2008). High-throughput tissue extraction protocol for NMR- and MS-based metabolomics. *Analytical Biochemistry*, *372*(2), 204–212. https://doi.org/10.1016/j.ab.2007.10.002

Wulfetange, K., Lomin, S. N., Romanov, G. A., Stolz, A., Heyl, A., & Schmulling, T. (2011). The Cytokinin Receptors of Arabidopsis Are Located Mainly to the Endoplasmic Reticulum. *Plant Physiology*, *156*(4), 1808–1818. https://doi.org/10.1104/pp.111.180539

Xie, D. X., Feys, B. F., James, S., Nieto-Rostro, M., & Turner, J. G. (1998). COI1: An Arabidopsis gene required for jasmonate-regulated defense and fertility. *Science*, *280*(5366), 1091–1094. https://doi.org/10.1126/science.280.5366.1091

Yonekura-Sakakibara, K. (2004). Molecular Characterization of Cytokinin-Responsive Histidine Kinases in Maize. Differential Ligand Preferences and Response to cis-Zeatin. *Plant Physiology*, *134*(4), 1654–1661. https://doi.org/10.1104/pp.103.037176

Zhu, X., Sun, L., Kuppu, S., Hu, R., Mishra, N., Smith, J., … Zhang, H. (2018). The yield difference between wild-type cotton and transgenic cotton that expresses IPT depends on when water-deficit stress is applied. *Scientific Reports*, *8*(1), 1–11. https://doi.org/10.1038/s41598-018-20944-7

Zwack, P. J., Rashotte, A. M., Zwack, P. J., & Rashotte, A. M. (2013). Cytokinin inhibition of leaf senescence Cytokinin inhibition of leaf senescence, *2324*(July). https://doi.org/10.4161/psb.24737